

“BABEȘ-BOLYAI” UNIVERSITY CLUJ-NAPOCA
DOCORAL SCHOOL OF APPLIED AND
THEORETICAL GEOLOGY

**Eocene (Bartonian) *Nummulites perforatus* accumulations
from the north-western part of the Transylvanian Basin:
taxonomic diversity, (bio)facies and depositional model**

Summary

PhD student
Szabolcs-Attila Kövecsi

Scientific advisor
Prof. Dr. Sorin Filipescu

Cluj-Napoca
2021

Keywords:

*Larger benthic foraminifera; paleoenvironment; biostratigraphy; Eocene; Transylvania Basin;
Romania;*

Contents

1. Introduction	1
1.1. Introductory notes.....	1
1.2. The structure, palaeoecology and biostratigraphy of larger benthic foraminifera (LBF).....	2
1.3. <i>Nummulites</i> accumulation: The state of the art	3
1.4. Previously proposed <i>Nummulites</i> accumulation facies models.....	4
1.5. Geological setting.....	4
1.5.1. Transylvanian Basin, Romania.....	4
1.5.2. Dorog Basin, Hungary	6
2. Paleontology and paleoecology	7
2.1. Introduction.....	7
2.2. Main facies of the studied sections	7
2.3. Material and methods	8
2.4. Results.....	8
2.5. Discussion	10
2.6. Taxonomic notes	12
2.7. Conclusions.....	13
3. Microfacies analysis and diagenetic features	15
3.1. Introduction.....	15
3.2. Material and methods	15
3.3. Results.....	15
3.4. Interpretation and discussion	18
3.5. Conclusions.....	20
4. Distribution of assemblages and depositional model	22
4.1. Introduction.....	22
4.2. Material and methods	22
4.3. Results.....	23
4.4. Discussion	25

4.5. Conclusions.....	30
5. Additional data provided by other fossil groups associated to the <i>Nummulites perforatus</i> accumulations.....	32
5.1. Calcareous nannoplankton	32
5.2. Smaller benthic foraminifera	38
5.3. Bryozoans.....	43
6. Conclusions.....	46
References.....	49

1. Introduction

1.1. Introductory notes

The genus *Nummulites* comprises a diverse fossil group of Paleogene benthic rotalid foraminifera which are common throughout the Neotethyan region (Schaub, 1981). Sedimentary successions made up almost exclusively of *Nummulites* tests are usually interpreted as nummulitic banks (Arni, 1965). These days, nummulitic accumulations extend from the West Pacific to the Central Mediterranean (Jorry et al., 2006) and form important hydrocarbon deposits in northern Africa, especially in Tunisia and Libya (Racey, 2001 and references therein; Jorry et al., 2006). However, despite their economic importance, the mechanisms which underlie the formation of these peculiar rock bodies remain debated.

Although these unique sedimentary bodies are well-developed within the northwestern region of the Transylvanian Basin, just a handful of papers have dealt with their palaeontology or other characteristics (Bombiță & Moisescu, 1968; Bombiță et al., 1975; Mészáros et al., 1987; Wanek et al., 1987; Bombiță, 1984; Papazzoni & Sirotti, 1995; Proust & Hosu, 1996; Bartholdy et al., 2000; Papazzoni, 2008; Papazzoni & Seddighi, 2018; Bindiu-Haitonic et al., 2021).

This PhD thesis deals with Eocene (Bartonian) *Nummulites perforatus* accumulations known from the northwestern part of the Transylvanian Basin. The aim of this work is to provide new and detailed information bearing on our knowledge of this peculiar sedimentary succession and to develop an integrated depositional model based on taxonomic, taphonomic, and sedimentological investigations.

The main objectives of this PhD research are therefore to:

- document *Nummulites* assemblages recovered from 18 studied sections;
- document and interpret the biofabrics observed in studied sections;
- document and interpret the sedimentological microfaciesal and diagenetical features based on thin-section analysis;
- quantify the A/B ratio of *Nummulites* assemblages;
- calculate shape variability for paleoenvironmental interpretations;
- categorize the test of the recovered *Nummulites* assemblages in light of their preservational state using the taphonomic scale proposed by Beavington-Penney (2004);
- discuss other fossil groups present in samples, including bryozoans.

1.2. The structure, palaeoecology and biostratigraphy of larger benthic foraminifera (LBF)

It is clear that the LBF are an extremely diverse group amongst foraminifera, including fossil and extant forms (Beavington-Penney & Racey, 2004). These taxa were abundant and widespread in shallow-water carbonates during the Upper Palaeozoic, Upper Cretaceous, and Cenozoic periods (Hallock, 1985; BouDagher-Fadel, 2008).

According to Loeblich & Tappan (1984), the genus *Nummulites* belongs to the Suborder Rotaliida. These organisms were extremely common and diverse during the Cenozoic (Racey, 2001) in shallow marine, warm, normal saline, and oligotrophic environments within the photic zone (Reiss & Hottinger, 1984). Extant examples of LBF live in tropical and subtropical shallow marine environments (BouDagher-Fadel, 2008); these organisms are important carbonate producers in modern reefs and other carbonate platform systems (Hohenegger, 2006). The Nummulitidae have flat planspiral, involute, or evolute tests or a combination of the two, and exhibit complex internal morphologies (Hallock & Glenn, 1986) with multilocular tests (Hohenegger et al., 2000), symmetrical around the equatorial section (Beavington-Penney & Racey, 2004). Test walls are constructed by regularly arranged, small rhombohedral calcite crystals with optical axes oriented perpendicular, or at 45°, to the surface (Beavington-Penney & Racey, 2004).

One of the most characteristic features of the genus *Nummulites* is test surface ornamentation. Five different types of ornamentation can be distinguished: (1) radiated; (2) sigmoidal; (3) meandriform; (4) reticulated, and; (5) postulated.

Characters including the proloculus, chambers, marginal cord, and the canal system in the marginal cord can be distinguished in terms of internal morphology (Fig. 1.1) (Beavington-Penney & Racey, 2004). Numerous groups of extant and fossil foraminifera have a sexually dimorphic life cycle, (Hollock, 1985; BouDagher, 2008). The trimorphic life cycle frequently observed in recent LBF populations is not seen in fossil assemblages (Mateu-Vicens et al., 2012). Indeed, in some recent LBFs, researchers have noted the presence of a third generation which produces megalospheric schizonts. It is also the case that examples of LBF have been used extensively since the 19th Century for palaeoenvironmental and biostratigraphic reconstructions (Papazzoni et al., 2017). Indeed, as a result of their rapid diversification and abrupt extinction, phylogenetic reconstruction is important for this lineage because LBF are excellent biostratigraphic markers (Schaub, 1981; Hollock, 1985).

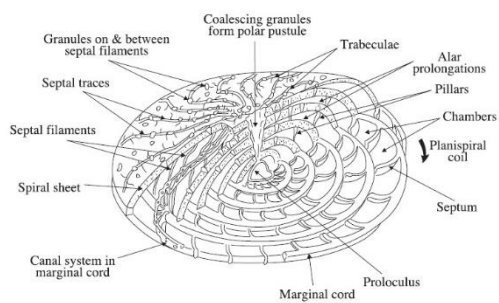


Fig. 1.1. The test structure of a megalospheric (A-form) *Nummulites* (taken from Beavington-Penney & Racey, 2004)

These evolutionary changes are due to symbiotic adaptations (Lee, 2006) which caused morphological changes within Nummulitidae from asymbiotic, small-sized ancestors to large and more complex forms.

The first biozonation for the Palaeocene-Eocene based on alveolinides, *Assilina* and *Nummulites* was given by Hottinger (1960) and Hottinger et. al. (1964). This initial biozonation was updated by Schaub (1981) and later by Hottinger and Drobne (1988). The present biostratigraphic zonation now used was established by Serra-Kiel et. al. (1998).

1.3. *Nummulites* accumulation: The state of the art

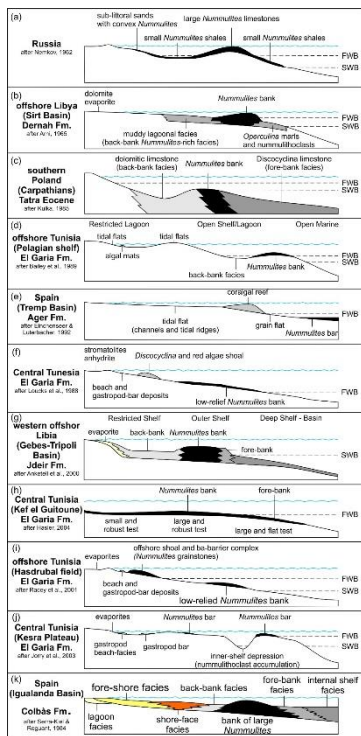
We know that *Nummulites* were the most abundant and widespread members of the biota in the Eocene oligotrophic warm Tethys Ocean and formed huge accumulations called “nummulites banks” (Arni, 1965). These peculiar sedimentary bodies are restricted to the Eocene Tethyan palaeo-margin (Racey, 2001).

In Arni’s (1965) model, these “nummulite banks” were interpreted as autochthonous deposits, comprised of one or two large *Nummulites* species including *N. gizehensis* or *N. perforatus* with large B-forms or low A/B ratios dominant.

This model was later questioned by Aigner (1985). He observed different biofabric structures induced by the hydrodynamic activity of the marine environment and conclude that “nummulite banks” are the results of consecutive winnowing, transporting, and sorting processes so that they hide para-autochthonous-to-allochthonous *Nummulites* tests. This latter observation made by Aigner (1985) instigated a long-lasting discussion regarding the autochthonous vs. allochthonous character of the “nummulite banks” (Papazzoni, 2008; Mateu-Vicens et al., 2012; Seddighi et al., 2015; Brigguglio et al., 2017).

Experimental studies on the hydrodynamic behaviour of larger foraminifera (Brigguglio et al., 2017) as well as taxonomic and individual counting (A/B ratio) studies (Papazzoni & Seddighi, 2018) have suggested a number of important features that characterise a “nummulite bank”.

1.4. Previously proposed *Nummulites* accumulation facies models



Several models have been proposed since the middle of the 20th Century to explain Eocene nummulitic accumulations (Fig. 1.2.). These models describe *Nummulites* accumulations as “nummulite bank”, bars, or low-relief banks related to palaeo-highs deposited from platforms- or shelf margins as far as the mid-to outer ramp environment.

Fig.1.2. Eocene facies models proposed for nummulitic accumulations. Models a-j modified after Jorjy et al. (2006) while model k was modified following Serra-Kiel & Reguant (1984).

1.5. Geological setting

1.5.1. Transylvanian Basin, Romania

The TB is one the representative sedimentary basin for the Paleogene of Romania (Fig. 1.3). The sedimentary record of the

basin is made of shallow marine and continental deposits.

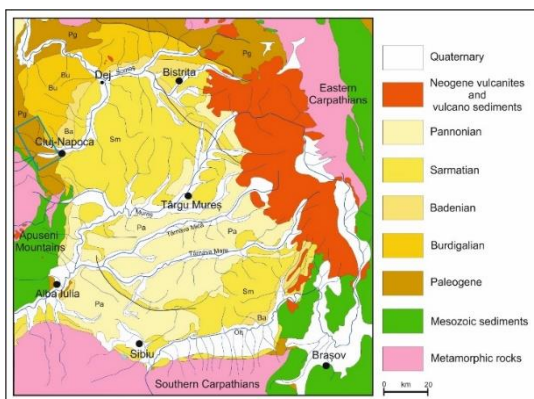


*Fig.1.3. Simplified geological map of the Transylvanian Basin modified after Filipescu (2011). The blue square marks the outcrop area of *N. perforatus* accumulations.*

Cenozoic evolution of the TB can be described by three succeeding depositional megasequences (Krézsek & Bally, 2006).

1. Paleogene Sag megasequence, which cover late Cretaceous formations. This megasequence consist of

alternating continental and marine deposition from the north-western and south-western parts of the basin.

2. Lower Miocene flexural megasequence, which consist of deep marine turbidites, coarse-grained fandelta, littoral sandstones, and outer shelf marls. Red continental and shallow marine deposits were documented in the southern part of the TB, as well.

3. Middle to upper Miocene back-arc megasequence, consisting a large-scale sedimentary succession from shallow marine to deep marine deposits. Overall, this is the thickest and extended megasequence in the TB.

The Eocene *Nummulites perforatus* accumulation which is the main subject of this thesis belongs to the lowermost Paleogene tectonostratigraphic megasequence (Krézsek & Bally, 2006).

The Căpuș Formation is a ~25 m thick stratigraphic record and consists of sands, clays, and limestones deposited in a shallow marine setting. It preserves mainly fossil assemblages of smaller and larger benthic foraminifera, but skeletal elements of marine phytoplankton, mollusks, ostracods, decapods, echinoids, and rare bryozoans also occur (Rusu et al. 2004; Kövecsi et al., 2016; Kövecsi et al., 2018; Bindu-Haitonic et al., 2021).

The nummulitic accumulation has an average stratigraphic thickness of 2-10 m (Rusu, 1987) and it can be studied at numerous exposures scattered on an area of ~200 km² located in the north-western part of the TB (Răileanu et al., 1968). This peculiar sedimentary record is often interpreted as nummulite bank (Papazzoni & Sirotti, 1995; Rusu et al., 2004; Papazzoni, 2008; Kövecsi et al., 2016) or shoal (Proust & Hosu, 1996) consisting of autochthonous to para-autochthonous *Nummulites* assemblages (Kövecsi et al., 2016; Pleș et al., 2020). The inferred paleoenvironment of these sedimentary successions is shallow water, an inner platform experiencing a relatively high energy regime (Papazzoni & Sirotti, 1995; Rusu et al., 2004) that was deposited in barriers and shoal facies (Proust & Hosu, 1996).

In addition to *Nummulites*, other fossil groups as smaller benthic foraminifera as well as calcareous nannoplankton, bryozoans, and ostracods are also present (Bombiță et al., 1975; Mészáros et al., 1987; Wanek et al., 1987; Kövecsi et al., 2018; Bindu-Haitonic et al., 2021).

Based on the paleontological record, the age of the *N. perforatus* accumulation is considered as early Bartonian. This age is suggested by the calcareous nannoplankton, which belongs to NP17/CP14 zones (Bindu-Haitonic et al., 2021) and by the presence of *N. perforatus*, which is the marker for SBZ 17 (sensu Serra-Kiel et al., 1998).

Studies on *Nummulites*-bearing deposits in the Transylvanian Basin date back in the 18th Century. The oldest published material about the *Nummulites* fauna from Transylvania was provided by Bruckmann (1727).

It is noteworthy that the type-locality of the species *N. perforatus* is located in the Transylvanian Basin, in the vicinity of Leghia. De Montfort (1808) described and illustrated the species *N. perforatus* as *Egeon perforatus* from this locality.

The outstanding work of Gheorghe Bombiță demarks the 20th century history of *Nummulites* research on the Transylvanian Basin. His research focused mainly on the biostratigraphy and taxonomy (see Bombiță, 1963, 1984; Bombiță & Moisescu, 1968) of the Transylvanian *Nummulites* fauna. More recent investigations were focused on different aspects of the *N. perforatus* accumulation as outlined by the works of Papazzoni & Sirotti (1995), Proust & Hosu (1996), Bartholdy et al. (2000), Papazzoni (2008), and Papazzoni & Seddighi (2018).

1.5.2. Dorog Basin, Hungary

The Eocene in the western part of the Dorog Basin corresponds to two major depositional sequences. The lower sequence (late Lutetian to early Bartonian) consists of the Dorog, Csernye and Csolnok formations and corresponds to the transgressive part of the Eocene (Less et al., 2000; Kercksmár, 2010). The lower Bartonian Tokod Formation represents the regressive part of the lower sequence. The Tokod Formation consists of greyish clayey marls with *Nummulites* at its base (Budai et al., 2008) and abundant mollusk shells in its lower part, which are covered by shallow-marine and fluvial sandstones interbedded with coal at the top. The nummulitic banks consist almost exclusively of well-preserved *N. perforatus* tests, although *Nummulites striatus* tests with the same preservation are sporadically present in the grey clayey matrix (Kercksmár, 1995). The nummulitic assemblage is indicative of the lower Bartonian SBZ 17 Zone of Serra-Kiel et al. (1998).

2. Paleontology and paleoecology

Chapter 2 is based on

Kövecsi S.,A., Silye L., Less G., Filipescu S. 2016. Odd partnerships among middle Eocene (Bartonian) *Nummulites*: Examples from the Transylvanian (Romania) and Dorog (Hungary) Basins. *Marine Micropaleontology*, 127: 86-98.

2.1. Introduction

Nummulitids are Cenozoic calcareous benthic foraminifera (Racey, 2001), which were abundant and widespread along the Neotethyan margin throughout the Eocene (Arni, 1965; Aigner, 1982, 1985; Papazzoni, 2008; Papazzoni and Seddighi, 2018). Deposits composed almost exclusively of one or rarely two species of *Nummulites* were called “nummulite bank” (Arni, 1965).

A special relationship between co-existing LBF species was documented by Hottinger (1999) and called “odd-partnership”. This term was introduced to define a relationship between two sympatric species, which bear structurally identical or very similar adult shells, but markedly differ in their protoconch and adult test size. The LBF assemblages offer the best examples in the fossil record or in recent habitats for the odd pairs. However, the existence of such a relationship between the highly diverse and stratigraphically important nummulitids has only been speculated, but never described (see Hottinger, 1999).

Our purpose was to describe in detail the first record of an ‘odd partnership’ in the case of middle Eocene (Bartonian) *Nummulites* species.

2.2. Main facies of the studied sections

The exposures studied in the Transylvanian Basin are usually a few meters high, and up to ~10–15 m wide and were logged and sampled at relatively high resolution (Fig. 2.1). The *Nummulites perforatus* accumulation of the Tokod Formation was sampled in a small outcrop in Bajót, Komárom-Esztergom County, Dorog Basin.

The most widespread sedimentary facies, structures and *Nummulites* biofabric-types observable at outcrop level are:

1. Shallow erosional scours filled with very weakly cemented nummulitic floatstone/rudstone.

2. Weakly cemented nummulitic rudstone/floatstone with chaotically stacked *N. perforatus* B-forms.

3. Nummulitic rudstone/floatstone with in contact or for imbricated *N. perforatus* B-forms.

4. Nummulitic floatstone with linear accumulation of *N. perforatus* B-forms.

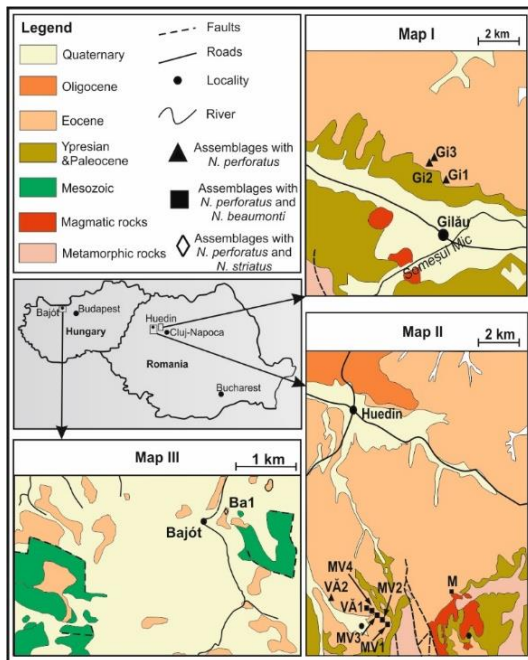


Fig. 2.1. Simplified geological maps of the studied area. Map I (Gilău area) and II (Huedin area) modified after Răileanu & Saulea (1968). Map III (Bajót area) modified after Budai & Síkhegyi (2005).

2.3. Material and methods

Twenty-six samples were collected from ten different outcrops (Fig. 2.1). One sample, was collected in Dorog Basin (Fig. 2.1). The collected samples were prepared following the standard micropaleontological preparation method. The biometrical measurements were performed on *Nummulites* A- and B-forms. In case of the A-forms 50 randomly selected specimens of *N. perforatus*, and all *N. beaumonti* and *N. striatus* specimens present in the studied residue (1/4 split) were measured per sample in order to record the diameter (D) and thickness (T) of their test. The internal diameter of the protoconch (C) was also measured on the equatorial split sections of the megalospheric (A) forms. On the *Nummulites* B-forms only the diameter (D) and thickness (T) were recorded. The A/B ratios were determined using 1 mm and 6 mm mesh sieves and only for the *N. perforatus*, because the other two taxa had a very low abundance.

2.4. Results

2.4.1. Identified assemblages and their geographic distribution

The *Nummulites*-assemblages recovered from the Eocene deposits of the Transylvanian Basin are markedly different in their species composition, and geographic distribution. Our investigation suggest, that in the easternmost located area, around Gilău, the LBF assemblages comprise only *N. perforatus*. However, about 25 km west of Gilău, around Huedin, the LBF assemblages consist mostly of *N. perforatus* in association with *N. beaumonti*. The LBF assemblage recovered from the Eocene of the Dorog Basin, situated far west from the Transylvanian Basin consists of *N. perforatus* in association with *N. striatus*.

2.4.2. Biometry of the studied *Nummulites* specimens

The average diameter (D) of the *N. perforatus* A-form specimens recovered from the Transylvanian Basin varies between 3.28 and 4.19 mm, and the thickness (T) between 1.89 and 2.55 mm. The values of *N. perforatus* A-forms from the Dorog Basin are of the same order of magnitude, although they are slightly higher: the average D is 4.20 mm, whilst the average T is 2.56 mm. *N. beaumonti* A-form specimens recovered only from the Transylvanian Basin have an average D between 1.63 and 2.34 mm, and a T between 0.68 and 1.43 mm, whereas the average D and T values obtained for *N. striatus* A forms from the Dorog Basin are 2.55 mm and 1.60 mm, respectively. The average T/D ratio of the *N. perforatus* A-forms is between 0.43 and 0.62, which is close to the average T/D ratio of the *N. beaumonti* (0.41–0.75)

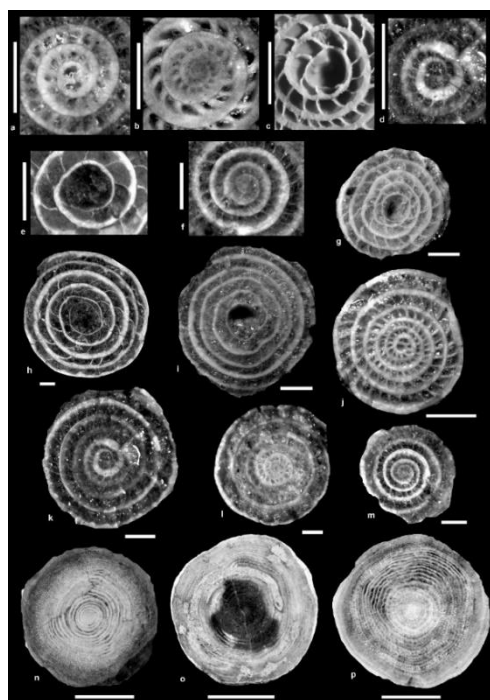


Plate 2.1. Photomicrographs of the studied *Nummulites* specimens. **a.** *Nummulites beaumonti* (d'Archiac & Haime) A form, sample MV2B; **b.** *Nummulites beaumonti* (d'Archiac & Haime) B form, sample MV3C; **c.** *Nummulites perforatus* (de Montfort) A form, sample VA1D; **d, k.** *Nummulites striatus* (Bruguière) A form, sample Ba1; **e.** *Nummulites perforatus* (de Montfort) A form, sample Ba1; **f.** *Nummulites striatus* (Bruguière) B form, sample Ba1; **g.** *Nummulites perforatus* (de Montfort) A form, sample M4; **h.** *Nummulites perforatus* (de Montfort) A form, sample Ba1; **i.** *Nummulites perforatus* (de Montfort) A form, sample G3; **j.** *Nummulites beaumonti* (d'Archiac & Haime) A form, sample MV1B; **l.** *Nummulites beaumonti* (d'Archiac & Haime) A form, sample VA1A; **m.** *Nummulites striatus* (Bruguière) B form, sample Ba1; **n.** *Nummulites perforatus* (de Montfort) B form, sample VA2A; **o.** *Nummulites perforatus* (de Montfort) B form, sample Ba1; **p.** *Nummulites perforatus* (de Montfort) B form, sample G3. Scale bars: a, b, d, f, k, i - 500 μ m; c, e, g, h, i, j - 1 mm, and n, o, p - 1 cm.

and *N. striatus* A-forms (0.64). The protoconch diameter (C) shows also large difference between the *N. perforatus* and *N. beaumonti* or *N. striatus* A-forms. The mean C of the *N. perforatus* A-forms varies between 780 and 927 μ m, whilst the mean C of the *N. beaumonti* A-forms is between 109 and 186 μ m. The LBF-assemblage from the Dorog Basin shows a similar difference between the mean C (920 μ m) of the *N. perforatus* A-forms, and the mean C (179 μ m) of *N. striatus* A-forms. The mean T/D ratio of the recovered *N. perforatus* B-forms is between 0.321 and 0.552.

2.4.3. A/B ratio of the *Nummulites* assemblages

The studied nummulitic assemblages have an A/B ratio between 15 and 135. In half of the outcrops, the A/B ratio decreases upwards. The minimum decrease of the A/B ratio was observed in outcrop Gi2, where this ratio decreases upsection from 70 to 39, whilst the maximum decrease

upsection (97 to 15) was recorded in exposure MV1. In other outcrops the A/B ratios increased upwards between 2 and 2.45 times, resulting in an increase of the A/B ratio from 54 to 106 (MV3) or from 35 to 86 (VA2). However the upward increase or decrease of the A/B ratio in the studied outcrops is not consistently related to any change of the biofabrics or sedimentary structures and the T/D of the *N. perforatus* B-form specimens is quite constant, even if the A/B ratio of the assemblages shows variability. In order to record the variations of the A/B ratio along the same stratigraphic level, the same strata were logged at different places. At the M outcrop the A/B ratio changed laterally along the strata from 39 (M1) through 112 (M2) to 47 (M4).

2.5. Discussion

2.5.1. Autochthonous or allochthonous assemblages?

The *Nummulites* A- and B-form specimens are well preserved. This is in good agreement with the most common *Nummulites* biofabrics observed in the Transylvanian and Dorog Basins. The chaotic stacking found in the nummulitic limestones is either interpreted as the result of wave action (Racey, 2001), or of bioturbation (Beavington-Penney et al., 2005). The presence of the shallow, wave related-scours supports the former interpretations, but where the scours are absent, the second interpretation cannot be ruled out. The decimetre scale linear accumulations of the *Nummulites* tests suggest parautochthonous wave or current winnowed accumulations (Aigner, 1985; Racey, 1995; Racey, 2001) or in situ compaction of the shells (Racey, 2001). The rarely observed imbrications are features related to unidirectional transport (Beavington-Penney et al., 2005), and they might be related to storm events (Beavington-Penney et al., 2006). The in situ position of the studied assemblages is supported by the floatstone facies observed on the outcrop level in some places, which is usually interpreted as a result of autochthonous accumulation, whilst the rudstone/floatstone facies present in other places might be the result of autochthonous/parautochthonous deposition (Racey, 2001). The presence of fine-grained, non-calcareous and not cemented sediment in the matrix of the floatstones and rudstone/floatstones observable in all studied exposures was regarded as a clear sign of the autochthonous deposition on the nummulitic banks in the Transylvanian Basin (Papazzoni, 2008).

Summarizing, based on the preservation state of the tests, the facies types and the lack of shape variability, we conclude that the studied nummulite banks in the Transylvanian and Dorog Basins preserve (para)-autochthonous (when imbrication is present) or autochthonous (any other case) assemblages deposited on a shore face.

2.5.2. Odd pairs within the nummulitic assemblages

There is a considerable test size difference between the *N. perforatus* A- and B-generations, however this does not apply for *N. beaumonti* and *N. striatus*. The specimens of the *N. beaumonti* and *N. striatus* had roughly half (A-forms) or one order of magnitude smaller (B-forms) adult test sizes than the A- and B-generation tests of *N. perforatus*. Such a considerable size difference between two species, which are taxonomically closely related, and share the same habitat can be interpreted as an ‘odd partnership’ sensu Hottinger (1999), or an ‘odd pair’ sensu Hottinger (2006). The observed co-occurrence of two taxa of the same genus with significantly different size in the Bartonian of the Transylvanian Basin, led us to define the *N. beaumonti* as the ‘San’ partner, and the *N. perforatus* as the ‘Don’ partner of such an odd pair. Based on the same observation regarding the size, co-occurrence and taxonomical affinity in the Bartonian of the Dorog Basin, we conclude that another odd pair can be defined there: the San partner is represented by *N. striatus* and the Don partner is *N. perforatus* as in the case of the odd pair observed in the Transylvanian Basin.

2.5.3. Paleoecology of the *Nummulites* odd pairs

Recent LBF live in symbiosis with photosynthetic algae (Haynes, 1965; Leutenegger, 1977; Hottinger, 1982; Leutenegger, 1984; Hallock, 1985; Lee & Hallock, 1987), and they are adapted to stable, tropical to warm-temperate, shallow marine, oligotrophic environments (Hottinger, 1983; Hallock, 1985). Because they depend on their symbionts and the amount of light necessary for those, they tend to develop tests with large surface/volume (Hohenegger, 2009), or small T/D ratio. Among recent LBF the occurrence of odd pairs is generally restricted to species living in the subtropical or tropical shallow marine upper photic zone. It is generally assumed that the species involved in odd partnerships have either different tolerance towards environmental conditions, as suggested by the odd pair *Adrosina lucasi* and *Archaias angulatus* (Levy, 1994), have different feeding modes (Lee et al., 1991), or reproduce in different periods (Zohary et al., 1980; Hottinger, 1999). The growth rate of the *Nummulites* can be very fast when multispiral growth is involved. For instance, *Nummulites millecaput*, which has the largest known test among *Nummulites*, could form a test with 10 cm diameter in not >5–6 years (Ferràndez-Cañadell, 2012). However, if multispiral growth is present, it is characteristic only for the microspheric B-forms, with the exception of two taxa: *N. perforatus* and *Nummulites cf. dufrenoyi*. *N. perforatus* B-forms always show this way of growing, whereas it is rare in A-forms (Schaub, 1981; Ferràndez-Cañadell, 2012). Consequently, the microspheric Don partners (i.e. *N. perforatus* B-form) of the studied odd pairs, most probably lived at least 2 years, based on their average diameter, and assuming a similar

growth rate as that of *N. millecaput*. The *N. perforatus* B-forms would eventually be able to reach their adult test size in the same amount of time as the twice smaller *N. beaumonti* and *N. striatus* A forms, if they had higher growth rate and/or a multispiral way of growing. The life span of the San partners *N. beaumonti* and *N. striatus* B-forms, which lack the multispiral growth, can be estimated to be about 1 year based on the longevity of the recent nummulitid *Operculina ammonoides* (Pecheux, 1995) and of *Amphistegina lobifera* (Triantaphyllou et al., 2012). The association of a single San partner *Heterostegina operculinoides* with two different Don partners has been already documented by Hottinger (1999).

Among the species taking part in these nummulitic odd pairs, the Don partner (i.e. *N. perforatus*) has the most frequent occurrence in the Bartonian (Schaub, 1981). Its association with two different San partners is not the result of its stratigraphic distribution, because both *N. beaumonti* and *N. striatus* occurred throughout the Bartonian (Schaub, 1981). The association of *N. perforatus* with two different smaller nummulitic species might be related to the more restricted paleogeographic distribution of *N. beaumonti* and *N. striatus* and/or to the different paleogeographic connections of the two basins. The distribution of the nummulitic odd pairs in the Transylvanian Basin reveals another feature. The San partners occur rarely in facies interpreted as a result of high-energy (wave or current dominated) action, whilst the Don partner's A- and B-forms are always present in these facies. This suggests, that *N. perforatus* was more adapted to variable environmental conditions than its San partners *N. beaumonti* and *N. striatus*.

The LBF and most of the known odd pairs are regarded as K-strategist species (Hottinger, 1997). Although the same can be thought for the Don and the San partners in the nummulitic odd pairs, we hypothesise, slightly different life strategies, because of the differences observable in their abundance, life span, mode of growing, and growth rate, occurrence, and palaeogeographic distribution. Along the r/K selection continuum, the larger, longer living, and more widely distributed Don partner could have been more K-strategist, than the smaller, shorter living, less widely distributed San partners.

2.6. Taxonomic notes

Oder Foraminiferida Eichwald, 1830

Family Nummulitidae Blainville, 1827

Genus *Nummulites* Lamarck, 1801

Nummulites perforatus (de Montfort, 1808) pl. 2.1, figs. c, e, g–i, n–p

- 1808 *Egeon perforatus* de Montfort – de Montfort, p. 167.
- 1853 *Nummulites perforata* d'Orbigny – d'Archiac & Haime, p.115–120, pl. VI, figs. 1–4.
- 1972 *Nummulites perforatus* (Montfort) – Blondeau, p. 161, pl. XXXIV, figs. 7–11.
- 1981 *Nummulites perforatus* (de Montfort) – Schaub, p. 88–90, figs. 76, 77, pl. 17, figs. 1–10, pl. 18, figs.1–31, pl. 19, figs. 1–8.
- 1995 *Nummulites perforatus* (de Montfort) – Papazzoni & Sirotti, p. 73, Pl I, figs. 7–8.

Nummulites beaumonti d'Archiac and Haime, 1853. pl. 2.1, figs. a–b, j

- 1853 *Nummulites Beaumonti* d'Archiac & Haime, p. 133–134, pl. VIII, figs. 1–3.
- 1883 *Nummulites sub-Beaumonti* de la Harpe – de la Harpe, p.182–183, pl. XXXI, figs. 48–56.
- 1981 *Nummulites beaumonti* d'Archiac & Haime– Schaub, p. 135–136, pl. 53, figs. 17–19, 22–25.
- 1995 *Nummulites beaumonti* d'Archiac & Haime – Papazzoni & Sirotti, p. 73, pl I, figs. 9–10.

Nummulites striatus (Bruguière, 1792).pl. 2.1, figs. d, f, k, m

- 1792 *Camerina striata* Bruguière – Bruguière, p. 399.
- 1853 *Nummulites contorta* Desh. – D'Archiac & Haime, p. 136–137, pl. 8, figs. 8 a, b.
- 1929 *Nummulina striata* Bruguière – Rozlozsnik, p. 194–195, pl. 6, figs. 6–7 and 20.
- 1981 *Nummulites striatus* (Bruguière) – Schaub, p. 153–154, pl. 53, figs. 26–31.

2.7. Conclusions

Three taxonomically closely related species have been observed in the autochthonous Bartonian *Nummulites* assemblages: *N. perforatus* and *N. beaumonti* were recovered from the Transylvanian Basin and *N. perforatus* and *N. striatus* from the Dorog Basin. The observed association between two closely related species, having very similar test morphology and structure but significantly different size was interpreted as an example of odd partnership sensu Hottinger (1999). The odd pairs formed by *N. beaumonti* as San and *N. perforatus* as Don partner (Transylvanian Basin), and that of *N. striatus* as San and *N. perforatus* as Don partner (Dorog Basin) likely lived in an oligotrophic, shallow marine environment within the upper photic zone. The association of the

same Don partner with two distinct San partners in two different sedimentary basins is interpreted as the result of the wider paleogeographic distribution, and more abundant occurrence of the Don partner (*N. perforatus*), as compared to *N. beaumonti* and *N. striatus*, the San partners. Our data suggest, that contrary to the odd partners known so far, in the otherwise K-strategist nummulitic odd pairs, the faster growing *N. perforatus* Don partner was more K-strategist, whilst the smaller San partners *N. beaumonti* and *N. striatus* were less K-strategists, and slightly more opportunistic.

3. Microfacies analysis and diagenetic features

Chapter 3 is based on

Pleș, G., **Kövecsi, S.A.**, Bindiu-Haitonic. R., Silye, L. 2020. Microfacies analysis and diagenetic features of the Eocene nummulitic accumulations from northwestern Transylvanian Basin (Romania). *Facies*, 66 (3), paper 20.

3.1. Introduction

The middle Eocene (Bartonian) sedimentary sequence in some areas of the Transylvanian Basin is characterized by relatively shallow-water bioclastic build-ups formed mainly by larger benthic foraminifera, mainly nummulitids (Popescu, 1978; Rusu et al., 2004; Kövecsi et al., 2016). This sedimentary record has variable thickness, lateral extent, biofabrics, and distribution throughout the basin. Coeval (Bartonian) deposits characterized by similar lithological, paleontological and sedimentary features are extremely rare within the Neotethyan realm (Papazzoni & Seddighi 2018), although the *Nummulites*, and the nummulitic limestones or accumulations are frequently present in the Eocene sedimentary record of the Neotethyan realm (Jorry et al., 2006 and references therein; Schaub, 1981). The present study is the first microfacies investigation of a poorly-cemented nummulitic accumulation of Transylvanian Basin. Its main objective is to highlight the importance of detailed thin-section-based analyses in the study of similar nummulitic accumulations.

3.2. Material and methods

The studied twenty-five samples were collected from three locations in the north-western part of the Transylvanian Basin (Fig.3.1). At each outcrop large oriented samples were collected from different levels of the nummulitic accumulations. Sample preparation was undertaken in the laboratories of the Department of Geology (Babeș-Bolyai University). The A- (macrospheric) to B-(microspheric) forms were point counted along each thin section using a binocular microscope.

3.3. Results

3.3.1. Outcrop description and sedimentological features

3.3.1.1. Manastirei outcrop

This outcrop is in the vicinity of the Mănăstireni village (Cluj County). Here a relatively thick sequence (approximately 2.5 meters thick) of poorly cemented nummulitic accumulations with a sandy detrital matrix is exposed. The lower part of the outcrop is characterized by chaotic stacking of nummulitid tests (Fig. 3.2). Few mollusk fragments (truncated bivalve shells) were present. In the middle part of the outcrop a discrete erosional surface can be distinguished, topped by a much coarser, densely packed bioclastic level with imbricated *Nummulites* B-forms (Fig.3.2). Towards the top, a well cemented highly compacted bioclastic level is present. Above this level, the facies are similar to that observed in the lower part of the sampled succession.

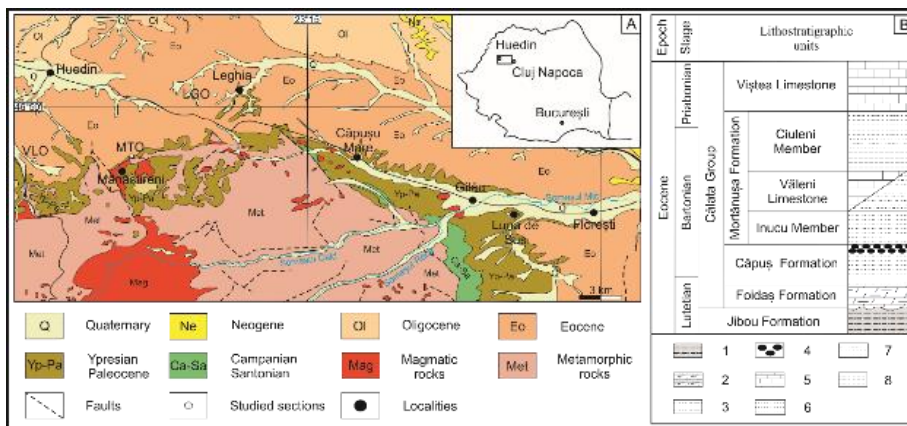


Fig.3.1. The location of the samples and regional stratigraphy: **A.** Simplified geological map of the studied area based on Răileanu & Saulea (1968); **B.** The Eocene lithostratigraphic units of the studied area (Rusu, 1995; Filipescu,

2001; Rusu et al., 2004): **1.** continental sedimentary record; **2.** claystone with marls; **3.** marlstones; **4.** nummulitic accumulation; **5.** limestones; **6.** claytones; **7.** sandy claystones; **8.** clayey sandstones.

3.2.1.2. Văleni outcrop

The second studied outcrop (VLO) is situated at the outskirts of Văleni village. The sampled sequence is represented by 1.7 meters thick, poorly cemented nummulitic accumulation similar to MTO. In the lower part of the outcrop, a clear dominance of chaotically stacked *N. perforatus* A-form specimens can be observed. They are embedded in a fine-grained clayey matrix succeeded by a level of densely packed *Nummulites* tests (Fig. 3.2). The middle part of the succession is marked by an erosional surface. Above this surface, levels of imbricated to linear stacked B-form *Nummulites* specimens interlayered with loosely arranged *Nummulites* A- and B-form tests were observed (Fig. 3.2).

3.3.1.3. Leghia outcrop (LGO)

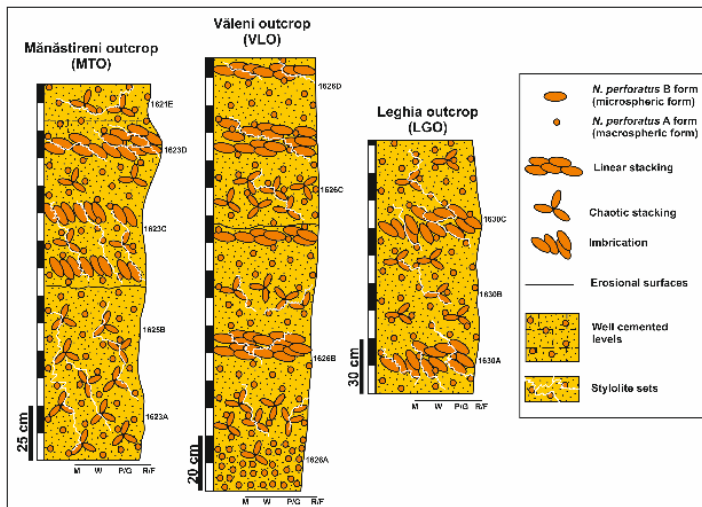
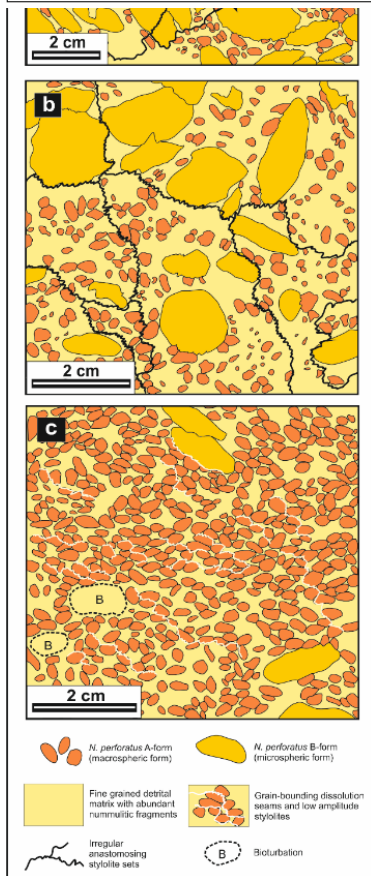


Fig. 3.2. Sedimentary logs of the studied sections

The Legia outcrop (LGO) is located in the vicinity of Leghia village. The outcrop consists of highly fractured and compacted nummulitic accumulations with a relatively poor cementation. Numerous sutured grains between the chaotically dispersed B-form *N. perforatus* tests are visible together with



abundant microstylolitic anastomosing sets. In the lower and middle part of the sampled succession, small levels of imbricated *Nummulites* tests can be sometimes noticed (Fig. 3.2). Bioerosional features are common. All nummulithoclasts are embedded, as observed in the previous outcrops, in a fine-grained detrital matrix.

Fig. 3.3 Schematic drawing of the main microfacies types (MFT1-3) established for the studied outcrops: **a** Densely packed nummulitic rudstone (MFT1); **b** Chaotically stacked nummulitic rudstone (MFT2); **c** Bioturbated nummulitic (A-form) rudstone (MFT3).

3.3.2. Microfacies analysis

3.3.2.1. Description of the main microfacies types

Three main microfacies types were established (MFT1-3) (Fig. 3.3). The densely packed nummulitic rudstone (MFT1) could be distinguished in all of the three outcrops. Chaotically stacked nummulitic rudstone (MFT2) and bioturbated nummulitic (A-form) rudstone (MFT3) were noticed only in MTO and VLO.

3.3.2.2. Biotic assemblages

The biotic assemblages in the studied outcrops are dominated by an outstanding number of densely packed *N. perforatus* specimens (A- and B-forms). Our microfacies analysis revealed that the matrix of these accumulations is made almost exclusively of fine nummulitic fragments.

Echinoid fragments were sometimes observed, mollusk fragments (bivalves) very scarce, whilst small benthic foraminifera were extremely rare within the detrital matrix.

3.3.3. A/B ratio of the *Nummulites perforatus* assemblages

The A/B ratio of the *Nummulites* assemblages is often used to constrain the autochthonous-allochthonous origin of the nummulitic accumulations or banks (Aigner, 1985; Kövecsi et al., 2016). In the studied outcrops the calculated A/B ratio of the *N. perforatus* assemblages is between 6 and 41. The highest A/B ratio (41) was present in the lowermost part of VLO while the lowest (6) was observed in the upper part of MTO.

3.4. Interpretation and discussion

3.4.1. Interpretation of the main facies types

3.4.1.1. MFT1- Densely-packed nummulitic rudstone

This microfacies represents the main microfacies type from the analyzed nummulitic successions. It was encountered in all of the three outcrops. It is defined by a relatively densely packed fabric of the main components (Fig. 3.3a) and numerous structures generated by pressure dissolution. In MTO the imbrication structures can be possibly associated with currents action (*sensu* Beavington-Penney et al., 2005) succeeded by intensive compactional processes. After burial, the lack of early marine cements and pressure dissolutions favored a selective removal of nummulithoclastic debris between the large nummulitic tests generating a much densely-packed fabric. Sutured seams, anastomosing stylolitic sets and concavo-convex contacts are the main observed traits of such processes within the imbricated levels of MFT1.

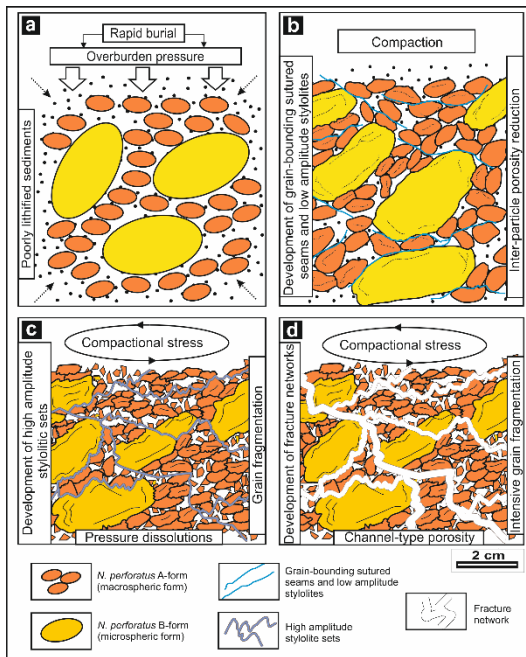
3.4.1.2. MFT2- Chaotically stacked nummulitic rudstone

The main feature of this microfacies type is the presence of numerous large, partly fragmented and bioeroded B-form *N. perforatus* tests. They are embedded in a fine-grained detrital matrix made almost exclusively of nummulitic fragments (Fig. 3.3b). The observed multi-grain sutured seams together with the low/high amplitude sets of stylolitic structures imply a high compaction degree generated by an overburden pressure prior to a progressive burial (see Alsharhan & Sadd, 2000; Toussaint et al., 2018).

3.4.1.3. MFT3- Bioturbated nummulitic (A-form) rudstone

Fig. 3.4. Proposed model of the stylolitization

phases within the studied nummulitic accumulation.



This main microfacies type was encountered only in VLO and is less well development within the sampled sedimentary record than MFT1 and MFT2.

The main feature of MFT3 is given by the presence of numerous A-form *N. perforatus* tests (Fig. 3.3c) embedded in a fine-grained bioturbated matrix. Even if the main nummulithoclasts developed a stacked pattern, the absence of high amplitude stylolite networks associated with fissures and cracks implies a lesser compaction degree in comparison to the other main microfacies types.

3.4.2. Diagenetic features and stylolitization phases

The presence of numerous stylolitic structures, fractures, sutured contacts between the main elements and a relatively high compaction degree are indicators of the burial diagenesis environment (Flügel, 2010; Toussaint et al., 2018). No evidence for the development of tectonically-related stylolites was observed. Taking into consideration that stylolitization is controlled by lithology and burial depth (Dunnington, 1967; Ben-Itzhak et al., 2014; Toussaint et al., 2018) the following aspects can be pointed out regarding the diagenetic history of the analyzed nummulitic accumulations. First, during the early stages of lithification, a rapid burial process started, which was responsible for the formation of numerous sutured dissolution seams and low amplitude stylolite sets (Fig 3.4a). Second, since most of the soluble sediments were affected by the previous stages of stylolitization the ongoing compactional stress triggered the development of fabric-selective high-amplitude rectangular/columnar stylolites (Fig. 3.4c). Third, despite the fact that the stylolitization reached a mature development stage, the succeeding compaction led to grain truncation and to the formation of a network of fractures/cracks (Fig3.4d).

3.4.3. Stylolitization impact on porosity and permeability

Studies focusing on the effects of pressure dissolutions in carbonate rocks concluded that the porosity and permeability are highly influenced by the stylolitization phases (Alsharhan & Sadd, 2000; Vandeginste & John, 2013; Ben-Itzhak et al., 2014; Toussaint et al., 2018). In all of the

sampled outcrops it was observed that the large amount of stylolite sets had gradually reduced the primary inter-particle porosity. However, the intra-particle porosity remained relatively high, especially within the *Nummulites* tests. Most probably the abundance of clay sediments within the nummulitic accumulations and the CaCO₃-poor fluids prohibited the formation of such pores along the dissolutional plane of the stylolitic structures.

3.4.4. Depositional paleoenvironment

Based on the grain supported fabrics, abundance of *N. perforatus* specimens embedded in a clayey detrital matrix and other sedimentary features, the formation of these bioaccumulations can most probably be related to a shallow-water inner-shelf paleoenvironment with hydrodynamic oscillations (Rusu et al., 2004; Kövecsi et al., 2016).

Considering that a bank or a build-up is a convex up structure, it can be deduced that the stylolites are more developed on flanks than on the crest because the increase in the pressure generated by the overburden stress. The rapid burial of the nummulitic accumulations can most probably be linked to transgression during deposition of the Căpuș Formation.

Regarding the autochthonous *versus* allochthonous nature of the *Nummulites* tests in the studied nummulitic accumulations Kövecsi et al. (2016) proposed an autochthonous and para-autochthonous state based on the identified biofabrics, the calculated A/B ratio of isolated *N. perforatus* specimens, and fossil content of the accumulations. The identified compactional structures provide additional support for this interpretation. In all of the sampled outcrops the large amount of micro-skeletal debris identified within and near the stylolitic seams therefore confirms this interpretation.

3.4.5. Interpretation of the A/B ratio

The observed variation of A/B ratios of the *Nummulites*-assemblages through the studied outcrops seems to be the result of the compaction processes. As the lower A/B ratios were encountered in samples/levels with clear evidence of compaction. However, our results suggest that the use of the A/B ratio might be problematic. The compactional processes after burial might have a considerable impact on the A/B ratio, resulting in low A/B ratio.

3.5. Conclusions

1. Thin section analysis revealed that a relatively high compactional stress generated a large amount of nummulithoclastic detrital particles and a well-developed network of stylolites and fractures in the nummulitic accumulations in the NW part of the Transylvanian Basin. Such

structures had a big influence on the development of textural heterogeneities, consolidation state and the morpho-structural peculiarity of the nummulitic accumulations. The pressure dissolution is an important clue to decipher the diagenetic history, porosity evolution and A/B ratio variations in *Nummulites* assemblages.

2. The morphological variability, orientation and development patterns of the stylolitic-fracture sets, together with other compactional features, imply a series of successive stylolitization phases that affected the nummulitic accumulations during burial diagenesis. The first phase was manifested through the genesis of numerous sutured dissolution seams as well as small, low amplitude stylolites during the early stages of lithification. The second stylolitization phase is represented by the development of fabric-selective interconnected rectangular microstylolites and high amplitude columnar stylolites that exhibit anastomosing patterns. The overburden pressure caused compactional damage as shown by grain truncation and the formation of an interconnected network of fractures associated with more mature stages of lithification.

3. Even though the pressure dissolution gradually reduced the primary intra-particle porosity, the stylolitic pathways favored the development of fracture systems which might considerably increase secondary porosity. The whole stylolite-fracture network can be interpreted as a three-dimensional percolation system, which improves the permeability and hence the reservoir potential of nummulitic accumulations.

4. The *Nummulites perforatus* A/B ratio variations in outcrops could also be related to these compactional features. Interesting is the fact that the lower A/B ratio values were obtained from the most compacted levels characterized by abundant stylolitic structures. Since most of the macrospherical A-forms are broken and fragmented, one may assume that such forms are more prone to fragmentation in comparison with the larger B-form *Nummulites*. Therefore, we assume that the compaction influenced the A/B ratio of nummulitic assemblages after burial.

5. The large amount of nummulithoclastic debris within and near the stylolitic networks developed around not or slightly abraded *Nummulites* tests supports the autochthonous or para-autochthonous nature of the analyzed accumulations. In addition, the fragmentation patterns of the B-form *N. perforatus* tests, together with numerous bioerosional structures, can be regarded as consequences of *in situ* pressure dissolution, rather than transportational abrasion.

6. The microfacies analysis proved to be a useful method in the study of large benthic foraminiferal accumulations. It provided a more accurate perspective on the internal morphostructural characteristics of the accumulation and also a better comprehension of the mechanisms involved in the evolution of the Eocene nummulitic build-ups in the Transylvanian Basin.

4. Distribution of assemblages and depositional model

Chapter 4 is based on

Kövecsi S.A., Less G., Bindiu-Haitonic R., Pleş G., Silye L., (submitted). *Nummulites* assemblages, biofabrics and sedimentary structures: the anatomy and depositional model of an extended Eocene (Bartonian) nummulitic accumulation from the Transylvania Basin (Romania).

4.1. Introduction

The nummulitic accumulations are essential component of the Eocene sedimentary record in the Neotethyan realm. They were mainly generated in the time interval when the Earth's climate experienced its warmest period in the Cenozoic (Zachos et al., 2008; Brandano & Tomassetti, 2021) and occurred in paleoenvironments interpreted as platforms, shallow-shelves or mid- to outer ramps (Racey, 2001). One of the key questions focuses on the autochthonous versus allochthonous origin of the *Nummulites* tests forming these build-ups. The first model of Arni (1965) suggested that the nummulitic accumulations rose due to the high reproduction rates of the in-situ *Nummulites* and low sedimentation rates of their habitat. Nonetheless, the autochthonous origin of the *Nummulites* tests found in nummulitic accumulations was questioned by Aigner (1982, 1983, 1985), who identified several sedimentary structures within these deposits and assigned them to winnowing and transport processes. Recently experimental data obtained on the hydrodynamic behavior of the LBF suggest that the development of the nummulitic accumulation is not only controlled by the waves or currents affecting a given habitat or by the ecological preferences of the main LBFs present in the nummulitic accumulation.

We present the first high resolution, 3D study focusing on the features of one of the largest spatially extended Eocene nummulitic accumulations in the northern part of the Neotethyan realm, and propose a paleoenvironmental model corroborated by paleontological and sedimentological data.

4.2. Material and methods

This work is based on the interpretation of sixty-two samples collected along eighteen outcrops of the nummulitic accumulation exposed between Cluj-Napoca and Huedin in the north-western part of the TB (Fig. 4.1). The sampled locations were described in detail with special care on the sedimentological structures and biofabrics observable on the field. The collected samples consist mainly of large, granular *N. perforatus* tests, rarely the small, radiate *N. beaumonti* (both A- and B-forms) are dominating. In some places the tests of both taxa occur in a muddy to sandy matrix.

Fossil remains of smaller benthic foraminifera, mollusks and bryozoans in low abundance are rather common (Kövecsi et al., 2016; Bindu-Haitonic, 2021).

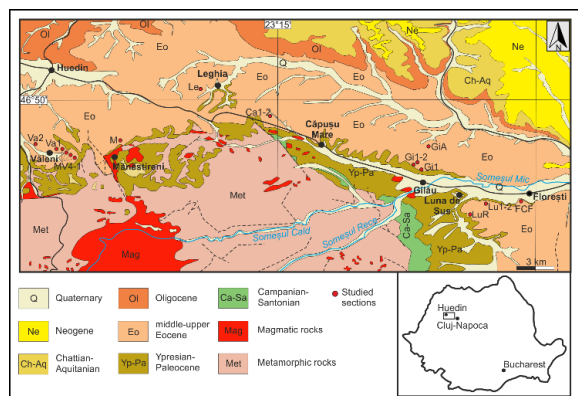


Fig.4.1. Simplified geological map of the studied area (based on Răileanu & Saulea 1968).

The samples were prepared in the laboratory following the standard micropaleontological preparation method. The dried > 63 μm residue was split in four, and ¼ part of each sample was used in further biometrical and taphonomical studies, and to estimate the ratio between the A- and B-form

(the A/B ratio) of the *Nummulites*-assemblages.

4.3. Results

4.3.1. Boundaries and bounding surfaces

The nummulitic accumulation overlain grey marls and it is covered by a ~ 10–15 cm thick bioclastic limestone with gastropods and bivalves.

The lower boundary of the nummulitic accumulation is sharp, not erosional and conformably covers the marls. In the marls rare small-sized *Nummulites* and smaller benthic foraminifera occur.

The nummulitic accumulation is covered by a 10–15 cm thick bioclastic limestone and highly calcareous marls (Inucu Member) deposited in an inner/outer-shelf setting (Mészáros & Moisescu, 1991; Rusu et al., 2004). The boundary between this unit and the upper part of the nummulitic accumulation is sharp and slightly erosional. A centimetre to decimetre-thick reddish level is observable just below this contact.

4.3.2. *Nummulites*-assemblages and associated biofabrics/sedimentary features

Three different *Nummulites*-assemblages could be recognized within the nummulitic accumulation based on the relative abundance of the LBF species and the A/B ratio of *Nummulites* assemblages.

4.3.2.1. Assemblage 1

This assemblage is dominated by *N. beaumonti* A- and B-forms, while *N. perforatus* A-forms are subordinate, and the B-forms are rare or missing. Assemblage 1 occurs in the northern and eastern part of the studied nummulitic accumulation, and was recovered from the base of GiA and LuR exposures, where the matrix supported or fine grained to coarse grained clast supported matrix

contains moderately preserved specimens of *N. beaumonti* and *N. perforatus* A- and B-forms. The *N. beaumonti* A-forms are subglobular while the rare B-forms are subglobular to inflated lenticular. The *N. perforatus* A-forms are inflated lenticular to lenticular, while the B-forms are lenticular in shape. The A/B ratio of the *N. beaumonti* specimens from this assemblage is between 34 and 42. When the *N. perforatus* B-forms is present, the A/B ratio of *N. perforatus* is 145. Assemblage 1 is associated to chaotic stacking biofabric (Fig. 4.2F).

4.3.2.2. Assemblages 2

It is the common *Nummulites*-assemblage observed along the studied nummulitic accumulation. This assemblage consists only of *N. perforatus* A- and B-forms and occurs almost all over the study area. In some places, mainly in the western part of the nummulitic accumulation, it alternates with Assemblage 3. The specimens assigned to this assemblage are embedded in matrix supported or fine grained to coarse grained clast supported matrix and are well preserved.

The *N. perforatus* A-forms are inflated lenticular, whilst the B-forms are inflated lenticular to lenticular. The A/B ratio of this assemblage is ranging from 27 to 176.

Several biofabrics could be recognized associated to the Assemblage 2. The most common biofabrics (Fig. 4.2A) are chaotic stacking and linear accumulations.

In some places contact and edgewise imbrications and erosional scours and fills are also observable (Figs. 4.2D, E). The fine-grained sediments from Lu1 and Lu2 are rich in glauconite.

4.3.2.3. Assemblages 3

This assemblage consists of abundant *N. perforatus* A- and B-forms, whereas *N. beaumonti* A- and B-forms are present but rare. It is less common than Assemblage 2, but occurs in almost all studied exposures of the nummulitic accumulation. The specimens of this assemblage are enclosed in a sandy, fine grained to coarse grained clast supported matrix. The *Nummulites*-tests are mainly well preserved. The *N. perforatus* A-forms are inflated lenticular, and the B-forms have inflated lenticular to lenticular shape. The recovered *N. beaumonti* A-forms are subglobular to inflated lenticular and the rare B-forms exhibit a subglobular to inflated lenticular shape. The A/B ratio of the *N. perforatus* is between 15 and 135, and in assemblages where *N. beaumonti* A-forms are present, the A/B ratio of the *N. beaumonti* specimens is 2 to 22.

The most common biofabrics observable in relation with Assemblage 3 are the chaotic stacking and linear accumulation of *N. perforatus* B-forms. In some places depositional features like erosional surfaces and current scours or current scours and fills could be recognized (Figs. 4.2A, B).

4.3.3. Paleoflow directions

The direction of paleocurrents could be determined in the western, central, and eastern part of the studied nummulitic accumulation (Fig. 4.3). In the western part the general dipping direction of the imbricated B-form *N. perforatus* tests indicates east-east-northeast paleocurrent direction (Fig. 4.3A). The imbricated *Nummulites* specimens retain an east-southeast paleoflow direction (Fig. 4.3B) in the central part of the nummulitic accumulation. The paleoflow directions in the eastern part of the studied sedimentary record point to east (Fig. 4.3 C) or to east-southeast (Fig. 4.3D), respectively.



Fig.4.2. Main facies and biofabrics. **A**-Chaotic stacking biofabric with coarse grain clast supported matrix (outcrop MV3); **B**-Current scours (outcrop LuR); **C**-Linear accumulations biofabric with matrix supported fabric and minor erosional surface (outcrop Va2); **D**-Current scour and fill (outcrop FCF); **E**-Imbricated biofabric with fine grained to coarse grained clast supported matrix (outcrop Le); **F**-Matrix supported fabric (outcrop GiA).

4.4. Discussion

4.4.1. The A/B ratio of the *Nummulites*-assemblages

The A/B ratio of the *Nummulites* A- and B-forms within a nummulitic assemblage is widely used as an important clue for the origin of the *Nummulites* tests within a nummulitic accumulation or to discriminate nummulite bank from non-nummulite bank (Papazzoni & Seddighi, 2018 and reference therein; Pleş et al., 2020).

The A/B ratio of the recovered *Nummulites* species displays values between 15 to 176 in case of *N. perforatus*, and 2 to 42 for *N. beaumonti*. The A/B ratio of the *N. perforatus* shows variations which is not related to the abundance of the taxa within an assemblage. The highest correlation coefficient (r^2) is 0.11 obtained between the mean D/T and A/B of the *N. perforatus* B-form. Focusing on the variability of the A/B ratio stratigraphically, it can be observed, that it has no clear pattern: sometimes is decreasing or has an increasing trend. Furthermore, any of these trends are not constantly related to any change in biofabrics, D/T ratio, or even facies. The A/B ratio recorded horizontally, along the same stratigraphic level show similar variability to that observed stratigraphically upwards. For example, on outcrop FCF the same stratum was logged laterally in 4 different points. Although the observed biofabrics are all over current scours and fills, the A/B

ratio has an increase from 16 to 59, and it has the best, but weak linear correlation ($r^2=0.42$) to the mean D/T values of *N. perforatus* B-form.

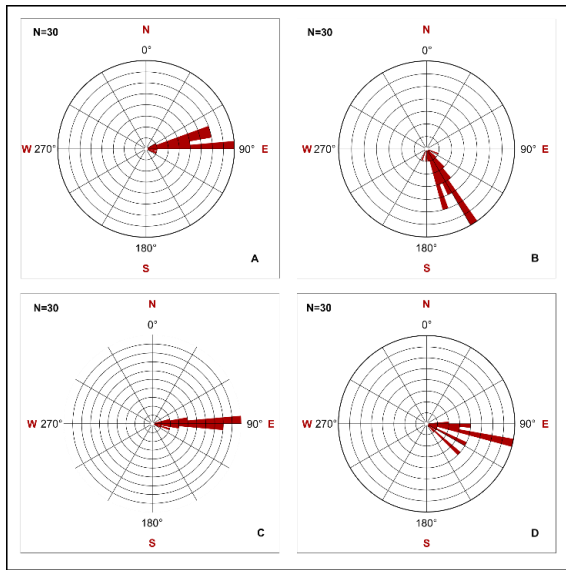


Fig.4.3. Rose diagrams of the paleoflow directions measured on the imbricated *Nummulites perforatus* B-form specimens. A-outcrop M, sample point M5; B-outcrop Le, sample point LeB; C-outcrop LuR, sample point LuRB; D-outcrop LuR, sample point LuRD.

The A/B ratio of the *N. beaumonti* shows clear differences between assemblages: it is the highest (42) in Assemblage 1 dominated by *N. beaumonti* while in Assemblage 3 with sporadic *N. beaumonti* it is only as low as 2–5 when only a few (3–6) specimens of this taxon occur in the assemblage.

Nummulites perforatus has the highest A/B ratio (145) or only *N. perforatus* A-forms are encountered in Assemblage 1 dominated not by *N. perforatus* but *N. beaumonti*. This can be explained either by population ecology or reproduction strategy or sedimentary processes. The lack of any correlation between the A/B ratio and D/T of *N. perforatus* or *N. beaumonti* in the assemblages suggest that the A/B ratio is not influenced by the energy, depth or turbulence of the depositional environment.

4.4.2. Interpretation of the identified *Nummulites*-assemblages

Assemblage 1 is interpreted here as autochthonous and represents the deepest part of the nummulitic accumulation. The autochthony of this assemblage is indicated by the dominance of TS1 state of preservation of the specimens, their chaotic stacking and the matrix supported or fine grained to coarse grained clast supported matrix. A further clue that they are in-situ is given by the co-occurrence of the smaller-size *N. beaumonti* and the larger *N. perforatus*. This type of co-occurrence called odd partnership is present only in assemblages preserved in-situ (see Kövecsi et al., 2016). The *N. perforatus* specimens of this assemblage are inflated lenticular to lenticular, while the B-forms lenticular inflated lenticular to lenticular (A-forms) or lenticular (B-forms), and have the highest D/T ratio encountered. These data compared to that of extant LBF, suggest a depositional environment slightly above the storm wave base (SWB) with low water-energy or an environment with decreased light conditions or water transparency, in the deepest part of the nummulitic accumulation (Hallock & Glen, 1986; Renema, 2005; Hallock & Seddighi, 2021).

Assemblage 2 is interpreted here as autochthonous to para-autochthonous assemblage deposited in shallower water than Assemblage 1 and with higher hydrodynamic regime. The mainly TS1

state of preservation of the specimens suggest that the studied material suffered transportation on a short distance by wave action or it was deposited in-situ. The short-distance transportation of at least some of the specimens is further supported by the decimetric sedimentary packets of edgewise or contact imbricated *Nummulites* tests.

This assemblage in some parts of the nummulitic accumulation is embedded in glauconite rich sediments (section Lu1, Lu2). The glauconite is either granular or pellicular. The morphology and the detailed mineralogy of the glauconite granules suggest that they are intrasequential (para-autochthonous) (Pop & Bedeleian, 1996).

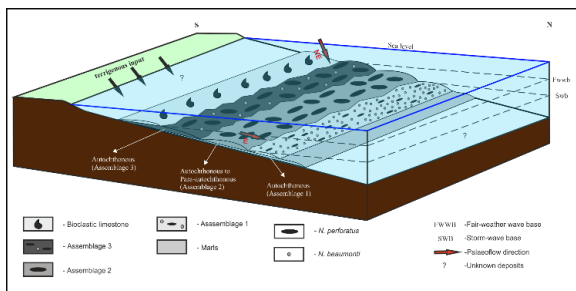
The shape of the *N. perforatus* specimens is inflated lenticular (A-form) or inflated lenticular to lenticular (B-form) and have a smaller D/T ratio than that of the specimens in Assemblage 1. Thus, Assemblage 2 was either deposited in a shallower part of the TB, somewhere between the fair-weather wave base (FWWB) and SWB with moderate water-energy or in an environment with increased light conditions or water transparency, compared to that experienced in the case of Assemblage 1 (Hallock & Glen, 1986; Renema 2005; Hallock & Seddighi, 2021).

Assemblage 3 is characterized by the dominance of the larger *N. perforatus*, and its co-occurrence with the smaller *N. beaumonti*. The co-occurrence of these two species of *Nummulites* is interpreted as odd partnership (sensu Hottinger, 1999). These types of co-occurrences are known from autochthonous fossil assemblages, and the autochthony was already demonstrated in the case of Eocene (Bartonian) *Nummulites* assemblages hosting odd pairs (Kövecsi et al., 2016; Briguglio et al., 2017). The *N. perforatus* A-forms are inflated lenticular, the B-forms have inflated lenticular to lenticular shape, and both are close in shape, but flatter than the associated smaller-sized *N. beaumonti* A-forms (subglobular to inflated lenticular) or B-forms (subglobular to inflated lenticular). The presence of fine-grained, non-calcareous, loosely matrix also points out the in-situ character of Assemblage 3 (Racey, 2001; Papazzoni, 2008; Briguglio et al., 2017). This interpretation agrees with the observed preservation of the *Nummulites* tests. Sedimentary features which can be attributed to extensive unidirectional currents (e.g. ripples) are absent and the most common biofabric is chaotic stacking of *N. perforatus* B-forms in the sedimentary record hosting the Assemblage 3. As the chaotic stacking is regarded to wave action (Racey, 2001; Beavington-Penney et al., 2005) or bioturbation (Beavington-Penney et al., 2005), the extensive transport can be ruled out. The second most frequently observed biofabric is the linear oriented *Nummulites* B-form. This type of biofabric is related to the in-situ compaction of the shells (Racey, 2001) or to wave or current winnowing (Aigner, 1985; Racey, 1995, 2001), further supporting the autochthony of Assemblage 3.

The average D/T ratio of the *N. perforatus* specimens is the lowest among the identified assemblages. This means that the *N. perforatus* A- and B-forms are the most inflated among the studied specimens. Therefore, we interpret this assemblage as deposited close to the FWWB, in a high water-energy environment, well within the photic zone (Hallock & Glen, 1986; Renema, 2005; Hallock & Seddighi, 2021).

4.4.3. Depositional model and evolution of the nummulitic accumulation

Fig.4.4. Depositional model of the middle Eocene (Bartonian) nummulitic accumulation from the northwestern part of the Transylvanian Basin, Romania.



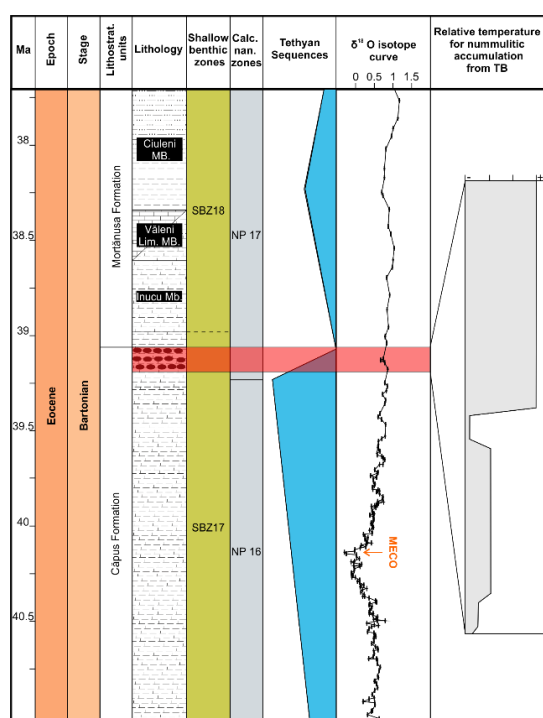
We integrated the features of the identified *Nummulites* assemblages, their stratigraphic and geographic distribution, the data on the taphonomy of the *Nummulites* specimens, and the observed sedimentological features, and propose herein a comprehensive depositional model for the middle

Eocene (Bartonian) nummulitic accumulation from the TB (Fig. 4.4).

The studied nummulitic accumulation represents a depositional record accumulated on a low angle inner shelf with low to high hydrodynamic regime, between the fair-weather and storm wave base. The observed transition between the identified assemblages is gradual or they sometimes alternate in space and time. However, a general trend of deepening towards north is interpreted based on the D/T ratio of the *Nummulites* specimens, their state of preservation, and the sedimentary features. The usual lack of any sign left by re-sedimentation phenomena suggests that the accumulation of the *Nummulites* tests was mainly controlled by biotic factors and not by sediment transport processes. The continuous development of the nummulitic accumulation on a large, shallow-water depositional setting in the TB excludes the massive re-sedimentation processes as well (Rusu, 1995). The three *Nummulites* assemblages and the measured paleoflow directions suggest the deepening of the paleoenvironment from S to N. Along the deepening gradient the major accumulation builders (*Nummulites* in this case) were changing their shape as a response to the environmental factor. Assemblages with small, thick *Nummulites* specimens indicate relatively shallow-water setting in the photic zone with or without high hydrodynamic regime, whilst the large, flat tests pinpoint deeper settings (Hallock, 1979; Hallock & Glenn, 1986; Hallock & Seddighi, 2021). This is also revealed by the observed change in the matrix. The locally observable imbrication, erosional scours or erosional scours and fills are attributed to the tidal currents or storm events (Beavington-Penney et al., 2006). Even so, imbricated biofabrics could

be generated by the in-situ compaction of the *Nummulites* tests (Pleş et al., 2020). The taxonomical and test's shape differences observed between the assemblages depend most probably on the environmental gradient changing accordingly with the water-depth along the nummulitic accumulation. Alternatively, the observed differences may reflect the distinct ecological parameters of the species co-occurring in Assemblages 1 and 3. Assemblage 1 occurs in the deepest, distal part of the accumulations, Assemblage 2 is restricted to the middle part of the accumulation. Assemblage 3 dominates the proximal, shallower part where seasonality might have had the heaviest impact on the assemblages .

The evolution of the nummulitic accumulation in the TB could be hypothesized and synthesized as follows: 1st phase: *N. beaumonti* and rare asexually generated *N. perforatus* propagules



colonized the substrate at around the SWB.

Fig.4.5. Tethyan sequences and oxygen $\delta^{18}O$ curve superimposed with available data on relative temperature curve of the nummulitic accumulation. Note the coincidence of sequence boundary and negative $\delta^{18}O$ excursion which coincide with the depositional time of the nummulitic accumulation from TB. Age, epoch, stage, Tethyan sequences after Gradstein et al. (2020), lithostratigraphy and lithology based on Kövecsi et al. (2018), shallow benthic zones Serra-Kiel et al. (1998), calcareous nannoplankton zones Martini (1971), $\delta^{18}O$ curve after Cramer et al. (2009) and relative temperature curve after Bartholdy et al. (2000).

This represents the birth of the nummulitic accumulation. The colonization was preceded by a relative sea-level rise resulting in a ravinement surface

in the sedimentary record (Proust & Hosu, 1996).

2nd phase: the development of the mass nummulitic accumulation or the main phase of the biotic accumulation. It is characterized mainly by the development of Assemblage 2 and by the less common appearance of Assemblage 3. They created a low-relief *Nummulites perforatus* build-up between the SWB and FWB in a sediment starving self or the rapid accumulation of the *Nummulites* test hampered the siliciclastic input. We assume that the habitat was characterized by the relative stability of the environmental conditions as reflected both by the smaller benthic foraminifera, LBF, and the glauconite sometimes occurring together with this assemblage. The $\delta^{18}O$ data of the *N. perforatus* tests (Bartholdy et al., 2000) collected from the interval (Fig. 4.5)

corresponding to this phase experienced a larger ($\sim 8\text{ }^{\circ}\text{C}$) seasonal temperature gradient and a slightly warmer water temperature ($\sim 25\text{ }^{\circ}\text{C}$).

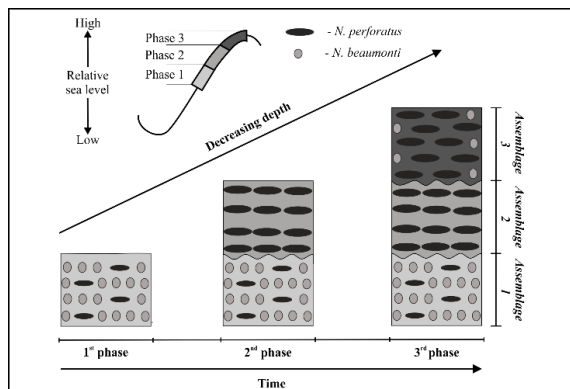


Fig.4.6. The inferred evolution of the nummulitic accumulation from the Transylvanian Basin.

We interpret these as clues for the shallowing. 3rd phase: as the shallowing of the habitat continued Assemblage 3 became more dominant and eventually it became the only LBF assemblage which could withstand the conditions around or above the FWB. The *Nummulites* odd-pair

indicate that the habitat was affected by strong ($\sim 10\text{ }^{\circ}\text{C}$) seasonality, and the recorded calcification temperatures (Fig. 4.5) reached the highest values ($\sim 29\text{ }^{\circ}\text{C}$) recorded (see Hottinger, 1999; Bartholdy et al., 2000; Kövecsi et al., 2016).

At the end of this phase the development of the nummulitic accumulation became very restricted or stopped because the relative sea-level rise reached the peak of the highstand (Fig. 4.6) and there was no further accommodation space available for its development (Proust & Hosu, 1996).

4.5. Conclusions

The nummulitic accumulation from the Transylvanian Basin comprises of autochthonous and autochthonous to para-autochthonous *Nummulites* assemblages, deposited on a low angle inner shelf between fair-weather and storm wave base.

The paleoenvironment had a deepening trend from S to N. Our results show that the studied nummulitic accumulation preserves three different *Nummulites* assemblages corresponding to three stages of the relative sea-level: Assemblage 1 consists almost entirely of *N. beaumonti* A- and B-forms, and rare *N. perforatus* A- and B-forms; Assemblage 2 consists exclusively of *N. perforatus* A- and B-forms; Assemblage 3 dominated by *N. perforatus* A- and B-forms with the co-occurrences of subordinate *N. beaumonti* A- and B-forms.

The development of the nummulitic accumulation resulted as the interplay between the biotic and abiotic factors. Thus, the relative abundance of different taxa reflects the interplay between the ecological preferences of the nummulitic accumulation generator two *Nummulites* species, basin (e.g., relative sea-level, and low sediment supply) and climate history. Consequently, the mono- or duo-specific nature of the *Nummulites* assemblages within the accumulations is interpreted primarily as the result of the ecological preferences and its interferences with the

environment, and secondly it reflects the ability of the *Nummulites* propagules to colonize new habitats. In the shallowest or deepest part of the nummulitic accumulation where the ecological conditions are “extreme” or less stable the assemblages are composed by two species but dominated by that one which was more adapted to the specific habitat. The assemblages are monospecific in the middle part of the nummulitic accumulation where the paleo-environmental conditions were the most stable.

5. Additional data provided by other fossil groups associated to the *Nummulites perforatus* accumulations

5.1. Calcareous nannoplankton

Sub-chapter 5.1 is based on

Bindiu-Haitonic R., Bălc R., **Kövecsi S.A.**, Pleş G., Silye L. 2021. In the shadow of giants: Calcareous nannoplankton and smaller benthic foraminifera from an Eocene nummulitic accumulation (Transylvanian Basin, Romania). *Marine Micropaleontology*, 165(101988).

and

Bindiu-Haitonic R., Bălc R., **Kövecsi S.A.**, Pleş G., Silye L. 2021. A dataset of calcareous nannoplankton and smaller benthic foraminifera from a middle Eocene nummulitic accumulation (Transylvanian Basin, Romania). *Data in Brief*, 36(107154).

5.1.1. Introduction

Data related on calcareous nannoplankton assemblages recovered from the *Nummulites perforatus* accumulation from TB are scarcely reported. Just few papers discuss its paleontological and biostratigraphical aspects (Bombița et al., 1975; Popescu et al., 1978; Geța, 1984; Rusu et al., 2004). A detailed study of calcareous nannoplankton that were associated to the larger benthic foraminifera communities on the palaeoenvironment of the nummulitic accumulation may offer a better view on the palaeoenvironment of the given sedimentary succession and can further constrain the age and palaeoecology of the fossil communities.

5.1.2 Material and methods

The nummulitic accumulation was sampled at high resolution: 21 exposures grouped around nine locations in the Gilău sedimentary area (hereafter GSA) and Meseș sedimentary area (hereafter MSA) of the Transylvanian Basin (see Fig. 5.1).

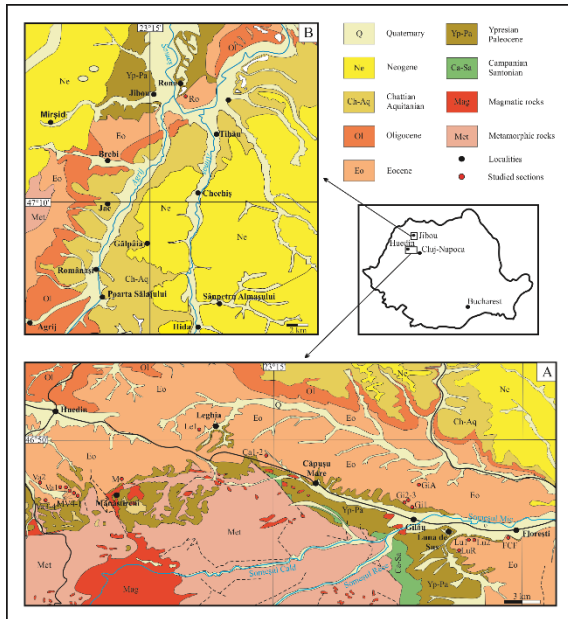


Fig.5.1. Simplified geological maps of the studied area: A- Gilău; and B- Meseș sedimentary area (after Răileanu & Saulea, 1968).

5.1.2.1 Investigation methods

Calcareous nannoplankton assemblages were investigated in 77 samples. Smear slides were prepared using the matrix between the *Nummulites* specimens following the standard smear slide technique. On every smear slide a minimum of 300 specimens were counted. Less calcareous nannoplankton rich samples were analyzed in 800

different fields of view. Calcareous nannoplankton taxa were classified according to online catalogue Nannotax 3. Quantitative data were obtained by counting at least 300 specimens per slide or, in the case of less abundant samples, all the specimens present in 800 different fields of view.

We correlated the samples to biozonation schemes developed for different latitudes due to the absence of the main marker species in our samples and to provide the most accurate age possible for the studied deposits.

Multivariate data analysis—hierarchical clustering and principal component analysis (PCA)—was performed to determine assemblages and the main taxa of the assemblages and responsible for the differences between assemblages. The calcareous nannoplankton taxa used for the multivariate data analysis were chosen based on the abundance of species and taxonomic groups and samples with <50 specimens were excluded from these analyses.

5.1.3 Results

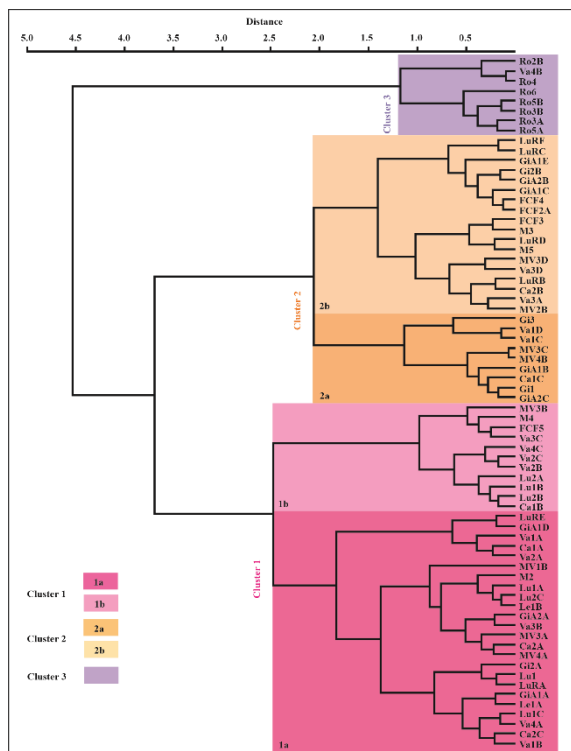
Forty-three calcareous nannoplankton taxa were identified in the studied samples, but some of the specimens could only be determined at the genus level due to their poor preservation. The calcareous nannoplankton assemblages are dominated by the following taxa: *Reticulofenestra umbilica*, *Reticulofenestra dictyoda*, *Blackites inflatus*, *Reticulofenestra minuta*, *Neococcolites dubius*, *Zygrabliothus bijugatus*, *Coccolithus pelagicus*, *Reticulofenestra daviesii* and *Ericsonia spp.* A clear difference between the samples from the southern and northern part of the nummulitic accumulation could be observed with respect to the diversity and abundance. The main differences are the higher number of *Micrantholithus spp.* and *Discoaster spp.*, the presence of *Sphenolithus*

predistentus and *Helicosphaera compacta*, the absence of *B. inflatus* and the lower abundance of *Ericsonia* spp., *N. dubius*, and *Z. bijugatus* in the MSA compared with the assemblages recovered from the GSA. The assemblages from the MSA have a higher number of taxa than those from the GSA, but the species richness of the assemblages is variable between samples and outcrops.

5.1.3.2 Cluster analysis

The dataset used for the cluster analysis is based on the main taxa (> ~2%). The multivariate hierarchical clustering grouped the samples (assemblages) into three clusters and four sub-clusters (Fig. 5.2). Cluster 1 consists of 35 samples and is divided in two sub-clusters. Sub-cluster 1a (*Zygrablithus–Neococcolithes* Assemblage) is characterized by a fluctuation in the abundance and intra-cluster shifts of the main taxa, showing a high variability of the relative abundance of species. Sub-cluster 1b (*Blackites–Ericsonia* Assemblage) groups the samples with the highest proportion of *B. inflatus*.

Fig.5.2. Grouping of the samples by clustering analysis (Ward's method) performed on calcareous nannoplankton assemblages.

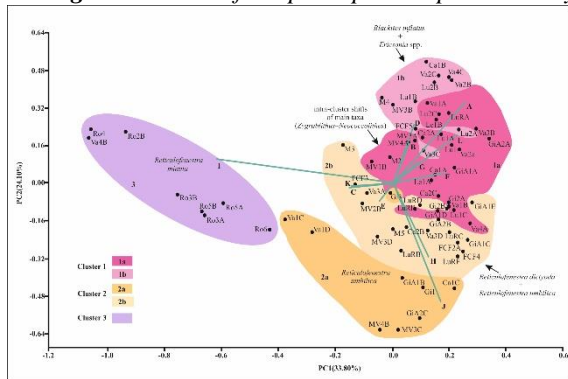


Cluster 2 groups 27 samples. Sub-cluster 2a (*Reticulofenestra umbilica* Assemblage) coincides with the highest proportion of *R. umbilica*. There is one exception (sample Gi3), which, apart from *Reticulofenestra* spp., has a higher percentage of *B. inflatus* and *C. pelagicus* than any other sample in this sub-cluster. Sub-cluster 2b (*Reticulofenestra dictyoda–R. umbilica* Assemblage) groups 18 samples with large reticulofenestrads. Cluster 3 (*Reticulofenestra minuta* Assemblage) includes eight samples with the highest proportion of *R. minuta* in association with other taxa (*Discoaster* spp., *Micrantholithus* spp. and *Sphenolithus* spp.) that are rare or absent in the rest of the samples. All

the samples, except Va4B, that are grouped into this cluster are from the Rona outcrop (MSA).

5.1.3.3 Principal component analysis

Fig.5.3. Results of the principal component analysis carried out on the selected calcareous nannoplankton taxa.



The first two principal components were found to be relevant (Fig. 5.3). They explain ~58% of the variability present in the relative abundance data of the main calcareous nannoplankton taxa. Principal component 1 explains 33.80% of the variance and contrast samples with *B. inflatus*, *N. dubius* and *Z. bijugatus* and those with *Discoaster* spp., *R. minuta* and *Sphenolithus* spp.. Principal component 2 retains 24.10% of the variance and separates the samples with *B. inflatus*, *C. pelagicus* and *Ericsonia* spp. from those with *R. dictyoda* and *R. umbilica*.

5.1.4. Biostratigraphy

The calcareous nannoplankton assemblages from the studied areas lack the main Eocene marker species and therefore their assignment to standard biozones is difficult. Bombiță et al. (1975) and Popescu et al. (1978) described an abundant calcareous nannoplankton assemblage from the Căpuș Formation and the nummulitic accumulation. They correlated this assemblage with the upper part of the NP15 and the lower part of the NP16 biozones of Martini (1971). This correlation is not in accordance with that of Gheța (1984), who created a regional zonation due to the absence of the index species of standard biozonations and correlated the nummulitic accumulation with the *Rhabdosphaera inflata* Zone. This, in turn, was correlated to the upper part of NP16 Zone (*Discoaster taninodifer* Zone) of Martini (1971). More recently, the nannofloral assemblages of the nummulitic accumulation-bearing Căpuș Formation were assigned to the NP16 Zone of Martini (1971) (Rusu et al., 2004). We therefore attempted to solve the problem of correlation between the standard nannoplankton zonations and the nummulitic accumulation based on our high-resolution sampling. The marker species are absent from the recovered assemblages. However, based on the presence and/or absence of some species (e.g., *R. umbilica*, *R. bisecta* and *Sphenolithus spiniger*) and their total range, the studied nummulitic accumulation was correlated with the Eocene (Bartonian) NP17 Zone (= CP14/CNE15/MNP17A Zone). This correlation fits well with that on larger benthic foraminifera (Kövecsi et al., 2016).

5.1.5. Palaeoenvironmental interpretations

The calcareous nannoplankton assemblages of the studied stratigraphic record can be separated in well-defined assemblages, as clearly evidenced by the results of the cluster and PCA analyses (Figs. 5.2 and 5.3). The samples collected from the nummulitic accumulation were grouped by the cluster analysis into three main clusters. Within each of two main clusters (Cluster 1 and 2), two sub-clusters (1a, 1b, 2a and 2b) could be identified. The PCA analysis further showed that these sub-clusters are grouped together and are separated along principal component 2 based on their *B. inflatus*, *Ericsonia* spp., *Z. bijugatus*, *N. dubius*, *C. pelagicus* and reticulofenestrid content. The *Zygrabliothus–Neococcolithes* Assemblage is a diverse assemblage with two dominant species. *Z. bijugatus* is often regarded as a eutrophic (Tremolada & Bralower, 2004; Villa et al., 2008) or oligotrophic (Wei & Wise Jr., 1990; Villa et al., 2008) taxon that prefers warm (Bralower, 2002; Melinte, 2005) or cool (Tremolada & Bralower, 2004) waters. It blooms in shallow (Monechi et al., 2000) or nearshore (Monechi et al., 2000; Melinte, 2005) environments or in deeper habitats (Aubry, 1998). Hence this assemblage suggests a nearshore, shallow marine, oligotrophic paleoenvironment with some pulsation of the nutrient content.

The *Blackites–Ericsonia* Assemblage consists mainly of three taxa. *B. inflatus* is abundant in shallow water to hemipelagic settings, but rare in pelagic sediments (Lowrie et al., 1982) or in poorly preserved assemblages (Agnini et al., 2014). *Ericsonia* spp. are regarded as K-strategist species adapted to temperate to warm waters and oligotrophic conditions (Bukry, 1973). *Coccolithus pelagicus* is considered to be either a temperate (Oszczypko-Clowes, 2001) or warm (Wei & Wise Jr., 1990) water species, although some researchers have interpreted it as a cold water species (Okada & McIntyre, 1979). This taxon prefers eutrophic (Rahman & Roth, 1990) or oligotrophic (Ozdínová & Soták, 2014) conditions and thrives in an environment with a high nutrient input (McIntyre & Bé, 1967) or a low influx of terrigenous material (Auer et al., 2014). Therefore, we regard this assemblage as reflecting a marine paleoenvironment with warm, shallow water, oligotrophic conditions and possibly with low influx of terrigenous material.

The *Reticulofenestra dictyoda–Reticulofenestra umbilica* and the *Reticulofenestra umbilica* Assemblages consist mainly of *Reticulofenestra* species. This group is abundant in temperate to high latitudes (Schneider et al., 2011) and prefers mesotrophic conditions (Villa et al., 2008). *Reticulofenestra umbilica* is a mesotrophic–oligotrophic species (Aubry, 1992) occurring in well-stratified seawater (Young, 1990) in a temperate climate (Wei & Wise Jr., 1990; Villa et al., 2008). As a result, these assemblages reflect the slightly different availability of nutrients and possibly a deeper environment than the previous assemblages. The *Reticulofenestra umbilica* Assemblage is regarded as reflecting a deeper and more nutrient-rich paleoenvironment than the *Reticulofenestra dictyoda–Reticulofenestra umbilica* Assemblage. The *Reticulofenestra minuta* Assemblage is

mainly restricted to the samples from the northern part of the nummulitic accumulation (Rona section), except one sample (Va4B). This species is associated with high-productivity eutrophic conditions, an increased influx of continental sediments and shows a tolerance to high environmental stress (Auer et al., 2014).

In conclusions the paleoenvironment in the northern part of the nummulitic accumulation was more eutrophic and probably deeper than in the south. This is also suggested by the changes in lithology toward more clayey strata, as well.

5.1.6. Conclusions

Our high resolution investigation carried out on the calcareous nannoplankton assemblages recovered from the studied sedimentary succession allow us to constrain the age and the palaeoecological changes within the *Nummulites perforatus* accumulations.

The obtained results can be summarised as follow:

1. 52 different species belonging to 21 calcareous nannoplankton genera were identified in the studied samples.

2. In the absence of the marker calcareous nannoplankton species, we should adopt the regional biozonation scheme proposed for the Bartonian deposits of the TB and to compare it with the standard biozonation schemes for this time interval. Thus, we correlate the nummulitic accumulation with the regional *Reticulofenestra bisecta* Zone and standard NP17/CP14 Zones.

3. Five calcareous nannoplankton assemblages were distinguished based on statistical analysis (cluster and PCA analysis). These are as follow: (1) *Reticulofenestra dictyoda*–*Reticulofenestra umbilica*; (2) *Reticulofenestra umbilica*; (3) *Reticulofenestra minuta*; (4) *Zygrablitus*–*Neococcolithes*; and (5) *Blackites*–*Ericsonina* and they are indicating different palaeoenvironmental conditions.

Hence the *Zygrablitus*–*Neococcolithes* Assemblage suggests a nearshore, shallow marine, oligotrophic palaeoenvironment with some pulsation of the nutrient content.

The *Blackites*–*Ericsonina* Assemblage reflects a marine palaeoenvironment with warm, shallow water, oligotrophic conditions and possibly with low influx of terrigenous material.

Reticulofenestra dictyoda–*Reticulofenestra umbilica* Assemblages and *Reticulofenestra umbilica* Assemblage reflects deeper environment and slightly different availability of nutrients than the previous assemblages, while the *Reticulofenestra minuta* Assemblage which is mainly restricted to the northern part indicates more eutrophic and deeper conditions than in the southern part of the studied nummulitic accumulations.

Based on the spatial distribution of the identified assemblages within the nummulitic accumulation a clear difference on the palaeoenvironmental condition can be observed. Thus a meso-oligothrophic palaeoenvironment was detected in the southern part and a more eutrophic palaeoenvironment in the northern part of the nummulitic accumulation.

4. The observed feature of the assemblages are mainly related to different factors as light intensity, nutrient supply, oxygen level and water depth and subordinately to biotic factors as competition with larger foraminifera.

5.2. Smaller benthic foraminifera

Sub-chapter 5.2 is based on

Bindiu-Haitonic R., Bălc R., **Kövecsi S.A.**, Pleş G., Silye L. 2021. In the shadow of giants: Calcareous nannoplankton and smaller benthic foraminifera from an Eocene nummulitic accumulation (Transylvanian Basin, Romania). *Marine Micropaleontology*, 165(101988).

and

Bindiu-Haitonic R., Bălc R., **Kövecsi S.A.**, Pleş G., Silye L. 2021. A dataset of calcareous nannoplankton and smaller benthic foraminifera from a middle Eocene nummulitic accumulation (Transylvanian Basin, Romania). *Data in Brief*, 36(107154).

5.2.1. Material and methods

Sixty-one samples grouped around 9 different locations were investigated for smaller benthic foraminifera (see Fig. 5.1 in chapter 5.1.2). The samples were prepared by the standard method. The residues were split with an ASC Micro Sample Splitter until an aliquot of about 200–300 benthic foraminifera specimens was obtained.

The smaller benthic foraminiferal counts were used to calculate paleoecological proxies and the benthic foraminifera dissolved oxygen index – BFOI (Kaiho, 1994). Multivariate data analysis as hierarchical clustering and principal component analysis (PCA) was performed to determine assemblages and main taxa of the assemblages to constrained the common traits and differences between assemblages. The smaller benthic foraminiferal taxa with $\leq 1\%$ relative abundance were excluded from further investigations.

The hierarchical clustering (Q-mode) was performed followed the method described in Chapter 5.1.2.1.

5.2.2. Abundance, assemblage composition, diversity and BFOI

The smaller benthic foraminifera are fairly abundant in the 63 μm to 1 mm fraction of the studied samples, but their preservation varies from poor to moderate. The number of smaller benthic foraminifera per gram varies from section to section and ranges between 12 and 1410 (Fig. 5.4A). Taxonomic analysis showed 46 smaller benthic foraminifera taxa belonging to 33 genera (Plates 5.2 and 5.3). In Ro, extremely rare and badly preserved planktonic foraminiferal specimens were present in the samples. A clear difference in the composition and abundance of the main specimens was observed between the southern (GSA) and northern (MSA) parts of the nummulitic accumulation. The most abundant taxa within samples from the GSA are *Pararotalia* spp., *Cibicides* spp., *Lobatula lobatula* and *Neoeponides* spp., whereas the dominant taxa in the samples from the MSA are *Protelphidium* spp., *Pararotalia* spp., *Cibicides heidingeri*, *Nonion* spp. and *Sagrinopsis* spp.. Therefore, the epifaunal forms dominate within the assemblages from the GSA (Fig. 5.4B), but along the Rona section (MSA) there are some overturns between the infaunal and epifaunal taxa. Fisher's alpha index and Shannon–Wiener diversity index record the minimum values in the samples from the southern part of the nummulitic accumulation and the maximum values in its northern part (Rona section) (Fig. 5.4C and D). The BFOI have values higher than 90, except for the samples collected from the northern part of the nummulitic accumulation (Ro outcrop) where they oscillate between 8.20 and 80.97 (Fig. 5.4E).

5.2.3. Cluster analysis

The multivariate clustering analysis (Ward's method) separated the assemblages into two main groups: cluster 1 and cluster 2. Cluster 1 is subdivided in two sub-clusters (1a and 1b) and cluster 2 into three sub-clusters (2a, 2b and 2c) (Fig. 5.5). Cluster 1 groups 23 assemblages belonging to seven exposures. *the studied outcrops reflects their geographic position.*

These are characterized by a moderate relative abundance of *Cibicides* sp., *C. heidingeri*, *Nonion* spp., *Pararotalia* spp. and *Protelphidium* sp. Sub-cluster 1a (*Protelphidium–Nonion* Assemblage) includes all the samples from the Rona outcrop (MSA). These yielded the assemblages with the highest proportion of *Protelphidium* sp. and *Sagrinopsis aspera* and are the only assemblages with agglutinated taxa. Sub-cluster 1b (*Cibicides* Assemblage) groups together the assemblages with the highest relative abundance of *Cibicides* sp., which is mostly associated with *Pararotalia* spp. and *L. lobatula*. Cluster 2 groups together the samples dominated by *Pararotalia byramensis*.

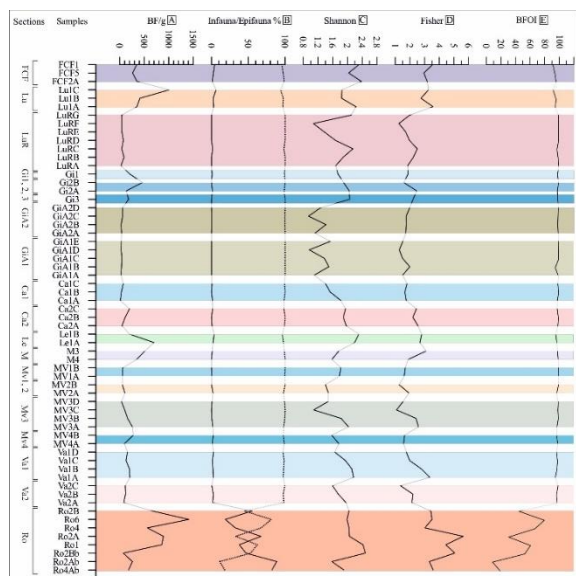


Fig. 5.4. (A) Abundance (density) of benthic foraminifera specimens per gram of sediment (B) Ecological preferences of benthic foraminifera (epifauna/infrauna). (C) Shannon's diversity index along the studied assemblages. (D) Fisher diversity index of the studied assemblages. (E) Benthic Foraminifera Oxygen Index (BFOI). Note: the colored rectangles are only used to separate the sections; the samples within a section are in stratigraphic order, and the order of the studied outcrops reflects their geographic position.

The samples grouped into Sub-cluster 2a (*Pararotalia byramensis*–*Cibicides haidingeri* Assemblage) are separated based on the high

percentages of *P. byramensis*, *C. haidingeri* and *P. subinermis*, together with *Neoeponides schreibersii* and *L. lobatula*. Sub-cluster 2b (*Pararotalia byramensis*–*P. subinermis* Assemblage) is defined by a high proportion of *P. byramensis* and *P. subinermis*. In the samples grouped in Sub-cluster 2c (*Pararotalia byramensis* Assemblage), *P. byramensis* records the highest relative abundance within the studied assemblage. It is associated with *Cibicides sp.*, while the rest of taxa sum to <9%.

5.2.4. Principal component analysis

The PCA analysis of the relative abundances of the benthic foraminifera was used to further corroborate the sample separation in groups by cluster analysis (Fig. 5.6). The first two principal component explain ~62% of the variability.

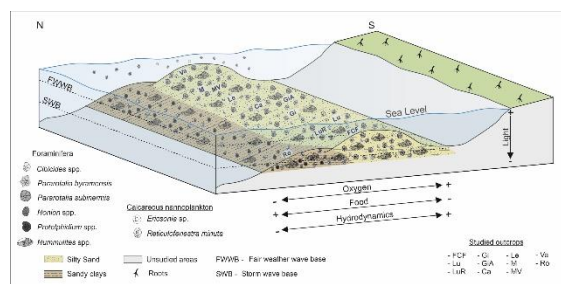
Principal component 1 retains 36.8% of the variance and separates samples with *Pararotalia spp.* from those dominated by *Protelphidium sp.*, *Nonion chapapotense*, *Nonion sp.*, *S. aspera* and *Tubulogenerina tubulifera*. Principal component 2 explains 24.9% of the variance and opposes the assemblages with a high proportion of *Cibicides sp.* and *L. lobatula* to the rest of them. Therefore, contrary to the cluster analysis, four different, more robust, sample groups of smaller benthic foraminiferal assemblages can be defined based on the principal components analysis: the *Protelphidium*–*Nonion*, *Cibicides*, *Pararotalia subinermis* and *Pararotalia byramensis* assemblages (Fig. 5.6).

5.2.5. Biostratigraphy

The recovered smaller benthic foraminifera taxa do not have biostratigraphic value except for *Pararotalia subinermis*, which is the marker species for the basin-scale Bartonian *Pararotalia*

These taxa have similar ecological preferences (Murray, 2006). They are known to be sessile, epifaunal, attached and their distribution is conditioned by the existence of suitable high-velocity bottom currents and hard or gravel-laden sediments (Murray, 2006). As a result, the *Cibicides* Assemblage can be interpreted as a clue for a shallow-water environment, with hard substrate, high velocity bottom currents, low nutrients and high dissolved oxygen levels. The *Protelphidium–Nonion* Assemblage is dominated by calcareous benthic taxa. *Pararotalia* spp. and *Cibicides* spp. are similar to those present in the smaller benthic foraminiferal assemblages in the GSA and suggest warm waters and shallow oligotrophic areas. *Pararotalia* spp. are less abundant in this assemblage. Important taxa include *Protelphidium*, *Nonion* and *Sagrinopsis*. Therefore, we regard the *Protelphidium–Nonion* Assemblage to live in a warm-water marine environment in the lower part of the photic zone, under high nutrients and low oxic conditions. The proportion of epifaunal/infaunal taxa (Fig. 5.4B) shows that the infaunal forms record high percentages in the samples from the Rona section, supporting the interpretation of the *Protelphidium–Nonion* Assemblage as reflecting a depositional environment below the wave base with a muddy substrate and eutrophic environmental conditions. The higher proportion of infaunal forms, together with the agglutinated and planktonic taxa, indicate deeper marine environments in the northern part of the nummulitic accumulation, although this area is still on the inner shelf (Fig. 5.7).

This is emphasized by the relatively high proportion of *Pararotalia* and *C. heidingeri* and by the thin lenticular *Nummulites* specimens toward the middle to upper parts of the outcrop. The



percentage of epifaunal specimens also increases toward the top of the exposure.

Fig.5.7. The distribution of the main calcareous nannoplankton and smaller benthic foraminiferal taxa along the nummulitic accumulation and the paleoenvironmental model of the Eocene nummulitic accumulation from the Transylvanian Basin.

5.2.7. Conclusions

The studied samples consist of diverse smaller benthic foraminifera assemblages. Ten genera of agglutinated, twenty-one genera of calcareous and one genus of porcelaneous foraminifera were identified on the studied material. Based on the recovered smaller benthic foraminifera assemblages and statistical analysis, the following conclusions can be drawn:

1. The identified smaller benthic foraminifera taxa do not have any biostratigraphic value except for *Pararotalia subinermis*. This is the marker species for the basin-scale Bartonian *Pararotalia*

subinermis Interval Zone. Hence the abundant presence of this species supports the Bartonian age of the *N. perforatus* accumulations.

2. Based on the statistical analysis, four well defined smaller benthic foraminifera assemblages (*Pararotalia subinermis*, *Pararotalia byramensis*, *Cibicides* and *Prothelphidium–Nonion*) were separated within the *N. perforatus* accumulations.

3. The *Pararotalia subinermis* and *Pararotalia byramensis* assemblages differ only at the species level. Hence based on the ecological preferences of the main taxa of these assemblages we interpreted them as clue for the photic zone, in a warm water, shallow muddy-sandy inner shelf, with low nutrient and high dissolved oxygen content in the water.

Based on the ecological preferences of the main taxa, the *Cibicides* Assemblages indicate shallow water, with hard substrate, high velocity bottom currents, low nutrient and high oxygen level palaeoenvironment.

The *Prothelphidium–Nonion* Assemblage was encountered just in the Rona section and differs clearly from the other defined smaller benthic foraminifera assemblages. Beside of the main taxa of this assemblage agglutinated benthic and planktonic taxa are present. Therefore, this assemblage reflects warm-water environment in the lower part of the photic zone, under high nutrients and low oxic conditions.

4. The spatial distribution of the four identified assemblages shows a clear shift along the palaeoenvironmental gradient through the nummulitic accumulations. Consequently, an oligotrophic environment can be assigned to the southern part and a more eutrophic environment to the northern part of the nummulitic accumulations.

5.3. Bryozoans

Sub-chapter 5.3. is based on

Kövecsi S.A., Zágoršek K., Filipescu S., Silye L. 2018. First report of *Kylonisa triangularis* Keij, 1972 (Bryozoa) from the middle Eocene (Bartonian). *Neues Jahrbuch für Geologie und Paläontologie Abhandlungen*, 289(3): 325-330.

A micropaleontological assemblage containing fossil bryozoans was recovered from the carbonate-siliciclastic Căpuș Formation (Popescu, 1978) which outcrops in the northwestern part of the Transylvanian Basin (Fig. 5.8). Previous studies on the Căpuș Formation have emphasized a range of subjects including sedimentology, litho-, and biostratigraphy (Koch, 1880; Papazzoni & Sirotti, 1995; Rusu, 1995; Proust & Hosu, 1996). Our recent investigations have also revealed the

presence of rare bryozoan fragments in the Bartonian nummulitic banks. This bryozoan assemblage is monospecific and consists of rare *Kylonisa triangularis* Keij, 1972 specimens. The material studied here was collected from the Bartonian Căpuș Formation located in the north-western Transylvanian Basin within the framework of our detailed studies targeting the *Nummulites perforatus* banks (Papazzoni & Sirotti, 1995; Rusu et al, 2004; Kövecsi et al., 2016).

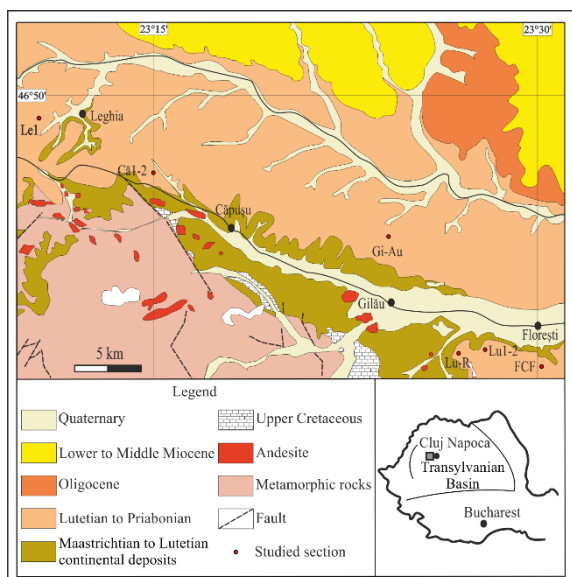


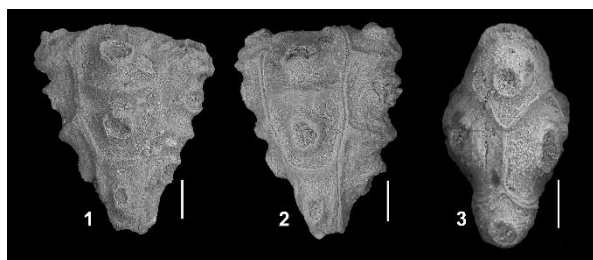
Fig.5.8. Simplified geological map to show the study area (after Răileanu & Saulea 1968) and location of this region within the Transylvanian Basin and Romania.

This sedimentary record consists almost exclusively of *N. perforatus* specimens and other rare fossil remains i.e. molluscs' fragments, bryozoan and small benthic foraminifera that are bound together by muddy to sandy matrix. Bryozoan remains were picked from randomly selected washing residue from each sample.

The bryozoan are rare in the studied samples. The relative abundance of bryozoans differs

along the nummulite bank from 1 to 58, probably as a result of taphonomic processes. This is also corroborated by variation in the state of specimen preservation and observed nummulite biofabric types sensu Aigner (1985). Sedimentary structures also indicate short to moderate transport.

The species *K. triangularis* has previously only known from southwestern France (Keij, 1972). The *Kylonisa* bearing sediments at both localities are middle Oligocene in age. In this paper we present new specimens of *K. triangularis* from the upper part of the Căpuș Formation (Transylvania Basin), a sequence which is middle Eocene (Bartonian) in age. We therefore hypothesize that *K. triangularis* first appeared earlier and originated east of the French occurrences. The Bartonian occurrence of *K. triangularis* within the Transylvanian Basin reported here supports our hypothesis, and further suggests that this species migrated from the east (Transylvanian Basin) towards the west (present-day southwestern France) during the Eocene/Oligocene along the northern margin of the closing Neotethys ocean.



Although the articulated colonies can be adapted to fine grained sedimentation because the branches are able to better shed the sediment **Plate.5.1.** SEM photographs of selected *K. triangularis*

specimens. 1- frontal view (sample Că2C); 2- oblique frontal (sample LuRC); 3- distal view (sample GiAu2D). Scale bar is 100 μm each.

than non-articulated colonies (Lagaaij & Gautier, 1965), paleoenvironmental interpretations of the *Kylonisa* bearing nummulitic banks known from the Transylvanian Basin, suggest that the *Kylonisa* colonies inhabited high energy shallow marine environments. The morphological features of the *Kylonisa* remains suggest that the living colonies were erect and flexible. Similar colonies are known from the Miocene and were interpreted as inhabiting shallow marine environment close to the wave base or in areas influenced by water currents (Key et al., 2013).

6. Conclusions

The present study is based on sixty-two samples collected along 18 sections from different parts of the Eocene (Bartonian) *Nummulites perforatus* accumulation located in the northwestern part of the Transylvanian Basin. The objective proposed for this study were to document the *Nummulites* assemblages recovered from the studied material, to document other fossil groups, to describe and interpret the sedimentological feature as biofabrics and microfacies types and in the and to propose a depositional model for this peculiar sedimentary body, based on the obtained micropaleontological and sedimentological data.

1. The taxonomical studies based on extensive biometrical analysis of the recovered *Nummulites* assemblages allow us to assign the identified populations to the species *Nummulites perforatus* as the main component within the nummulitic accumulation, and *Nummulites beaumonti* as less frequent component. These findings are in contrast with the data of Bombiță (1984) who reported higher diversity *Nummulites* assemblages from this sedimentary unit.

2. The observed co-occurrence of *N. perforatus* and *N. beaumonti*, with very similar test morphology and structure but different test size, suggests an odd partnership sensu Hottinger (1999), assigning *N. perforatus* to Don, while *N. beaumonti* to San partner. The most common nummulitic biofabrics observed within the studied nummulitic accumulation are the chaotic stacking, linear orientation and imbrication of the B-form *N. perforatus*. The distribution of these biofabrics along the studied sections and the presence or missing of odd pairs within the samples, suggests a para-autochthonous (when just the Don partner and imbrications are present) or autochthonous (any other case) origin for the studied *Nummulites* assemblages. So far, the nummulitic odd pairs were interpreted as K-strategists. Our data suggest that the Don partner (*N. perforatus*) was more K-strategist, while San partner (*N. beaumonti*) was less K-strategist and more opportunistic. This conclusion is based on the wider paleogeographic distribution and more abundant occurrence of Don partner compared as the San partner.

3. The recovered *Nummulites* assemblages estimated A/B ratio is between 15 and 135. The observed variation is not related to any change of the biofabric or sedimentological structure. Consequently, the observed variability is not related to any transportation or winnowing processes, suggesting that other factors like population ecology or reproduction strategy could influence the A/B ratio of the *Nummulites* assemblages. Based on the individual counting of the A and B-forms performed on the thin sections the obtained A/B ratio is between 6 and 41. The lower A/B ratio values were from the most compacted levels characterized by abundant stylolitic structures. Since most of the A-forms are broken and fragmented, we may conclude that those forms are more prone

to fragmentation than the large B-form *Nummulites*. Consequently, we assume that compaction could influence the original A/B ratio of the *Nummulites* assemblages after burial.

4. Microfacies analysis suggests that the studied nummulitic accumulation suffered a high compactional stress, which generated a large amount of nummulithoclasts detrital particles, well developed stylolite networks, and fractures. The above-mentioned structures had an important influence on the development of textural heterogeneities, consolidation states and morphostructural features preserved on the nummulitic accumulation. The observed pressure dissolution seems to be an important clue which influenced the diagenetic history, porosity evolution and A/B ratio variation of the *Nummulites* assemblages.

The development of the stylolitic-fractures sets, the morphological variability, the development patterns and other compactional features refer to at least two successive stylolitization phases that affect the nummulitic accumulation during burial diagenesis. The huge amount of nummulithoclastic debris within and near the stylolitic networks developed around not or slightly abraded *Nummulites* test supports the autochthonous or para-autochthonous origin of the studied *N. perforatus* accumulation. Additionally, the observed fragmentation degree on the B-form *N. perforatus* test and numerous bioerosional structures can be related as a consequence of in situ pressure dissolution, followed by transportational abrasion.

5. The detailed paleontological and sedimentological analysis performed on the Eocene (Bartonian) *N. perforatus* accumulation from the north-western part of the TB, allowed the identification of three different *Nummulites* assemblages deposited on a low angle inner shelf with low to high hydrodynamic regime, between the fair-weather and storm wave base. The assemblages correspond to three different phases within the relative sea-level changes. Assemblage 1 is dominated by A and B-form *N. beaumonti* and subordinate *N. perforatus* A-forms. The *N. perforatus* B-forms are rare or entirely missing. Assemblage 2 consists exclusively of A- and B-form *N. perforatus*, while Assemblage 3 is characterized dominantly by A- and B-forms of *N. perforatus* and rare A- and B-form of *N. beaumonti*.

The assemblages' composition observed biofabric and associated sedimentological features suggest that Assemblage 1 and 3 preserve autochthonous *Nummulites* assemblages, while Assemblage 2 might be considered to preserve autochthonous to para-autochthonous assemblage.

The development of the nummulitic accumulation is a result of the interplay between the biotic and abiotic factors. Hence the taxonomic content and relative abundance between the assemblages reflects the ecological preferences of the two identified taxa (*N. perforatus* and *N. beaumonti*), basin and climate history. Consequently, the mono- or duo-specific nature of the identified assemblages is interpreted as influenced by the ecological preferences and their interferences with

the environment and the ability of the *Nummulites* propagules to colonize new habitats. In the deepest and shallowest part of the nummulitic accumulation, where the ecological conditions were “harsh”, instable or affected by seasonality, the assemblages are composed by two species but dominated by the one more adapted to the specific habitat. The monospecific assemblages developed in the middle part of the nummulitic accumulation where the paleo-environment was more stable.

6. The calcareous nannoplankton and smaller foraminifera assemblages suggest progressive changes of the environmental conditions along the nummulitic accumulations from south to north.

Hence the southern part of the nummulitic accumulations is characterized by meso-oligotrophic conditions, while the northern part by a more eutrophic palaeoenvironment.

7. The calcareous nannoplankton belongs to the regional *Reticulofenestra bisecta* Zone and standard NP17/CP14 zones of the Bartonian. The smaller benthic foraminifera have been assigned to the Bartonian *Pararotalia subinermis* Interval Zone, therefore we have a good control on the Bartonian age of the nummulitic accumulations.

8. Taxonomic investigation performed on 33 samples from 9 different localities revealed the presence of rare *Kylonisa triangularis* Keij, 1972 (Bryozoa) specimens. This bryozoan species has been known so far from southwestern France (Keij, 1972). Previous to our finding the *K. triangularis* bryozoan, was known so far from middle Oligocene deposits. With its presence in middle Eocene deposits we hypothesize that *K. triangularis* first appeared earlier than middle Oligocene and migrated from east (Transylvanian Basin) to west (southwestern France) during the Eocene/Oligocene transition.

Based on the morphological characters of the *Kylonisa* fossils, we concluded that the living colonies were erect and flexible and they most probably lived in shallow marine environment influenced by water currents.

9. Our material is characterized by a various micropaleontological content, which allowed a fair reconstruction of the palaeoenvironment and palaeoecological conditions at the level of the *N. perforatus* accumulations. The autochthonous to para-autochthonous *Nummulites* assemblages were deposited in a low angle inner shelf setting, between the fair weather wave base and storm wave base, characterized by meso-oligotrophic conditions in south and eutrophic conditions in north. The composition of the nummulitic accumulations seems to be the results of the interplay between the biotic and abiotic factors.

References

- Agnini, C., Fornaciari, E., Raffi, I., Catanzariti, R., Pälke, H., Backman, J., Rio, D., 2014. Biozonation and biochronology of Paleogene calcareous nannoplanktons from low and middle latitudes. *Newsletter on Stratigraphy*, 47(2): 131-181.
- Aigner, T., 1982. Event-stratification in nummulite accumulations and in shell beds from the Eocene of Egypt. In: Einsele, G., Seilacher, A. (eds.) – *Cyclic and Event Stratification*. Springer Berlin Heidelberg, Berlin, pp. 248-262. <https://doi.org/10.1016/j.pgeola.2018.08.003>.
- Aigner, T., 1983. Facies and origin of nummulitic buildups: an example from the Giza Pyramids Plateau (Middle Eocene, Egypt). *Neues Jahrbuch für Geologie und Paläontologie*, 166(3): 347-368.
- Aigner, T., 1985. Biofabrics as dynamic indicators in nummulite accumulations. *Journal of Sedimentary Research*, 55(1): 131-134. <http://doi.org/10.1306/212f86342b2411d78648000102c1865d>.
- Alsharhan, A., Sadd, J., 2000. Stylolites in Lower Cretaceous carbonate reservoir, U.A.E. *Society for Sedimentary Geology Special publication*, 69: 185-207 <https://doi.org/10.2110/pec.00.69.0185>.
- d'Archiac, A., Haime, J., 1853. Description des animaux fossils du groupe nummulitique de l'Inde. Précédée d'un résumé géologique et d'une monographie des *Nummulites*. Gide et Baudry, Paris, 409 pp.
- Arni, P., 1965. L'évolution des Nummulitinae en tant que facteur de modification des dépôts littoraux. *Mémoires du Bureau de Recherches Géologiques Minières*, 32: 7-20.
- Aubry, M.P., 1992. Late Paleogene calcareous nannoplankton evolution: a tale of climatic deterioration. In: Prothero, D.R., Berggren, W.A. (eds.) - *Eocene–Oligocene Climatic and Biotic Evolution*. Princeton University Press, Princeton, NJ, pp. 272-309.
- Aubry, M.P., 1998. Early Paleogene Calcareous nannoplankton evolution: a tale of climatic amelioration. In: Aubry, M.-P., et al. (eds.) - *Late Paleocene–early Eocene Biotic and Climatic Events in the Marine and Terrestrial Records*. Columbia University Press, New York, pp. 158-201.
- Auer, G., Piller, W.E., Harzhauser, M., 2014. High-resolution calcareous nannoplankton palaeoecology as a proxy for small-scale environmental changes in the early Miocene. *Marine Micropaleontology*, 111: 53-65.
- Bartholdy, J., Bellas, Spyridon, M., Keupp, H., Anatol, R., Hosu, A., 2000. Oxygen and carbon isotope paleontology and paleoecological conditions in nummulitic banks: First results from the Transylvanian Eocene. *GFF*, 122(1): 21-22. <http://dx.doi.org/10.1080/11035890001221021>.
- Beavington-Penney, S.,J., 2004. Analysis of the effects of abrasion on the test of palaeonnummulites venosus: implications for the origin of nummulithoclastic sediments. *Palaios*, 19: 143-155. [http://dx.doi.org/10.1669/08831351\(2004\)019<0143:AOTEOA>2.0.CO;2](http://dx.doi.org/10.1669/08831351(2004)019<0143:AOTEOA>2.0.CO;2).
- Beavington-Penney, S.,J., Racey, A., 2004. Ecology of extant nummulitids and other larger benthic foraminifera: applications in palaeoenvironmental analysis. *Earth-Science Reviews*, 67: 219-265. <http://dx.doi.org/10.1016/j.earscirev.2004.02.005>.
- Beavington-Penney, S.,J., Wright, V.P., Racey, A., 2005. Sediment production and dispersal on foraminifera-dominated early Tertiary ramps: the Eocene El Garia Formation, Tunisia. *Sedimentology*, 52: 537-569. <http://dx.doi.org/10.1111/j.13653091.2005.00709.x>.
- Beavington-Penney, S.,J., Wright, V.P., Racey, A., 2006. The Middle Eocene Seeb Formation of Oman: an investigation of acyclicity, stratigraphic completeness, and accumulation rates in shallow marine carbonate settings. *Journal of Sedimentary Research*, 76: 1137-1161. <http://dx.doi.org/10.2110/jsr.2006.109>.
- Bindiu-Haitonic, R., Bălc, R., Kövecsi, S.A., Pleş, G., Silye, L., 2021. In the shadow of giants: calcareous nannoplankton and smaller benthic foraminifera from an Eocene nummulitic accumulation (Transylvanian Basin, Romania). *Marine Micropaleontology*, 165: 101988. <https://doi.org/10.1016/j.marmicro.2021.101988>.
- Blainvill, H.M.D., 1827. *Manuale de malacology et de conchyliologie (1825)*. F.G. Levrault, Paris
- Blondeau, A., 1972. *Les Nummulites*. Vuibert, Paris, 254 pp.
- Bombiță, G., 1963. *Contribuții la corelarea eocenului epicontinental din R.P. Română*. Editura Academiei Republicii Populare Romine, București, 113 pp.
- Bombiță, G., 1984. Le Napocien, vingt ans après sa définition. *Revue de Paléobiologie*, 3 (2): 209-217.

- Bombiță, G., Gheța, N., Iva, M., Olteanu, R. 1975. Éocène moyen-supérieur et Oligocène inférieur des environs de Cluj. In "Guide micropaleontologique Mésozoïque Tertiaire Des Carpates Roumaines" Institut Géologie Géophysique Roumaine, 163-174.
- Bombiță, G., Moiesescu, V., 1968. Données actuelles sur le Nummulitique de Transylvanie. *Mémoires du Bureau de Recherches Géologiques et minières*, 58: 693-729.
- BouDagher-Fadel, M.K., 2008. *Evolution and Geological Significance of Larger Benthic Foraminifera*, Elsevier, 544 pp.
- Bralower, T.J., 2002. Evidence of surface water oligotrophy during the Paleocene–Eocene thermal maximum: nanoplankton assemblage data from Ocean Drilling Program Site 690, Maud Rise, Weddell Sea. *Paleoceanography and Paleoclimatology*, 17(2): 1029-1042.
- Brandano, M., Tomassetti, L., 2021. MECO and Alpine orogenesis: Constraints for facies evolution of the Bartonian nummulitic and Solenomeris limestone in the Argentina Valley (Ligurian Alps). *Sedimentology*. <https://doi.org/10.1111/sed.12829>.
- Briguglio, A., Seddighi, M., Papazzoni, A.C., Hohenegger, J., 2017. Shear versus settling velocity of recent and fossil larger foraminifera: New insights on nummulite banks. *Palaios*, 32(5): 21-329. <http://dx.doi.org/10.2110/palo.2016.083>.
- Bruckmann, F.E., 1727. *Specimen Physicum sistens Historiam naturalem lapidis nummalis transylvaniae*. Wolfenbuttelae, 17 pp.
- Bruguière, M., 1792. *Encyclopédie Méthodique ou par ordre de matières*. Histoire Naturelle des Vers. Panckoucke, Paris. 344 pp. <http://dx.doi.org/10.5962/bhl.title.8638>.
- Budai, T., Császár, G., Csillag, G., Fodor, L., Gál, N., Kercsmár, Z., Kordos, L., Pálfalvi, S., Selmeczi, I., 2008. Geology of the Vértes Mts. Explanatory Book to the Geological Map of the Vértes Hills (1:50 000). Geological Institute of Hungary, Budapest.
- Budai, T., Síkhegyi, F., 2005. Geological Map of Hungary, 1:100.000, Dorog (Esztergom) Hungarian Geological Institute, Budapest.
- Bukry, D., 1973. Low-latitude coccolith biostratigraphic zonation. *Initial Reports of the DSDP 15*, 685-703.
- Cramer, B. S., Toggweiler, J. R., Wright, J. D., Katz, M. E., Miller, K. G., 2009. Ocean overturning since the Late Cretaceous: Inferences from a new benthic foraminiferal isotope compilation. *Paleoceanography*. 24: PA4216, doi:10.1029/2008PA001683.
- Dunnington, H.V., 1967. Aspects of diagenesis and shape change in stylolitic limestone reservoirs. *Proceedings of World Petroleum Congress 7th, Mexico*, 2: 339-352.
- Eichwald, C.E., von, 1830. *Zoologia specialis*. Pars altera, Vilnae, 233 pp.
- Ferrández-Cañadell, C., 2012. Multispiral growth in *Nummulites*: paleobiological implications. *Marine Micropaleontology*, 96-97:105-122. <http://dx.doi.org/10.1016/j.marmicro.2012.09.001>.
- Filipescu, S., 2001. Cenozoic lithostratigraphic units in Transylvania. In: Bucur, I.I., Filipescu, S., Săsăran, E. (eds.), *Algae and carbonate platforms in western part of Romania. 4th Regional Meeting of IFAA Cluj-Napoca 2001 - Field Trip Guidebook*. Cluj University Press, pp. 75-92.
- Filipescu, S., 2011. Cenozoic lithostratigraphic units in Transylvania. In: Bucur, I. & Săsăran, E. (eds.) - *Calcareous algae from Romanian Carpathians*, Presa Universitară Clujeană, pp 37-48.
- Flügel, E., 2010. *Microfacies of Carbonate Rocks. Analysis Interpretation and Application*. Second Edition, Springer, Berlin Heidelberg, pp. 984.
- Gheța, N., 1984. The Eocene of Transylvania. A new biostratigraphic interpretation. *Dări de Seamă ale Institutului, Seria Geologie-Geofizică*, 69(3): 95-106.
- Gradstein, F.M., Ogg, J.G., Schmitz, M.D., Ogg, G.M. (eds.) *Geologic Time Scale 2020*, pp. 1357, Elsevier.
- Hadi, M., Mosaddegh, H., Abbassi, N., 2016. Microfacies and biofabric of nummulite accumulations (Bank) from the Eocene deposits of Western Alborz (NW Iran). *Journal of African Earth Sciences*, 124: 216-233. <http://dx.doi.org/10.1016/j.jafrearsci.2016.09.012>.
- Hallock, P., 1985. Why are larger foraminifera large? *Paleobiology* 11:195-208. <http://dx.doi.org/10.2307/2400527>.
- Hallock, P., Glenn C.E., 1986. Larger foraminifera; a tool for paleoenvironmental analysis of Cenozoic carbonate depositional facies. *Palaios*, 1(1): 55-64. <https://doi.org/10.2307/3514459>.

- Hallock, P., Seddighi, M., 2021 Why did some larger benthic foraminifera become so large and flat? *Sedimentology*. <https://doi.org/10.1111/sed.12837>.
- de la Harpe, P., 1883. Monographie der in Aegypten und der libyschen Wüste vorkommenden *Nummulites*. *Palaeontographica*, 30:155–216.
- Haynes, J.R., 1965. Symbiosis, wall structure and habitat in foraminifera. *Contributions from Cushman Foundation for Foraminiferal Research*, 16:40-43.
- Hohenegger, J., 2006. The importance of symbiont-bearing benthic foraminifera for West Pacific carbonate beach environments. *Marine Micropaleontology*, 61(1-3): 4-39. <https://doi.org/10.1016/j.marmicro.2006.05.007>.
- Hohenegger, J., 2009. Functional shell geometry of symbiont-bearing benthic Foraminifera. *Galaxea, Journal of the Coral Reef Studies*, 11:81-89. <http://dx.doi.org/10.3755/galaxea.11.81>.
- Hohenegger, J., Yordanova, E., Hatta, A., 2000. Remarks on west Pacific Nummulitidae (Foraminifera). *Journal of Foraminifera Research*, 30: 3-28. <https://doi.org/10.2113/0300003>.
- Hottinger, L., 1960. Recherches sur les Alvéolines du Paléocène et de l'Éocène: *Schweizerische Paläontologische Abhandlungen*, 75-76: 1-253.
- Hottinger, L., 1982. Larger foraminifera, giant cells with a historical background. *Naturwissenschaften*, 69:361-371. <http://dx.doi.org/10.1007/BF00396687>.
- Hottinger, L., 1983. Processes determining the distribution of larger foraminifera in space and time. *Utrecht Micropaleontological Bulletins*, 30: 239-253.
- Hottinger, L., 1997. Shallow benthic foraminiferal assemblages as signals for depth of their deposition and their limitations. *Bulletin de la Société Géologique de France*, 168:491–505.
- Hottinger, L., 1999. “Odd partnership”, a particular size relation between close species of larger foraminifera, with an emendation of an outstandingly odd partner, *Glomoalveolina delicatissima* (Smout, 1954), Middle Eocene. *Eclogae Geologicae Helveticae*, 92:385-393. <http://dx.doi.org/10.5169/seals-168680>.
- Hottinger, L., 2006. Illustrated glossary of terms used in foraminiferal research. *Carnets de Géologie / Notebooks on Geology-Memoir*, 2: 1-126.
- Hottinger, L., Drobne, K., 1988. Alvéolines tertiaries: Quelques problèmes liés à la conception de l'espèce. *Revue de Paléobiologie*, 2: 665-685.
- Hottinger, L., Lehmann, R., Schaub, H., 1964. Données actuelles sur la biostratigraphie du Nummulitique Méditerranéen. *Mémoires du Bureau de Recherches Géologiques et minières*. 28: 611-652.
- Jorry, S., Hasler, C.-A., Davaud, E., 2006. Hydrodynamic behaviour of *Nummulites*: implications for depositional models. *Facies*, 52: 221–235. <http://dx.doi.org/10.1007/s10347-005-0035-z>.
- Kaiho, K., 1994. Benthic foraminiferal dissolved-oxygen index and dissolved oxygen levels in the modern ocean. *Geology*, 22: 719-722.
- Keij, A.J., 1972. *Sylonica* and *Kylonisa*, two new Paleogene bryozoan genera (Cheilostomata, Skylloniidea). *Scripta Geologica*, 11: 1-15.
- Kercsmár, Z., 1995. *A Tatabányai medence keleti peremének öskörnyezeti rekonstrukciója és tektonosedimentológiai vizsgálata*. Master dissertation, Department of Paleontology. Eötvös Lóránd University, Budapest, p. 120.
- Kercsmár, Z., 2010. Eocene stratigraphy of the N-Gerecse. In: Wanek, F., Gagy, P.A. (eds.) - *XII. Conference on Mining, Metallurgy and Geology*. Hungarian Technical Scientific Society of Transylvania, pp. 148-153.
- Key, M.M.Jr., Zágoršek, K., Patterson, W., 2013. Paleoenvironmental reconstruction of the Early to Middle Miocene Central Paratethys using stable isotopes from bryozoan skeletons. *International Journal of Sciences*, 102(1): 305–318. <http://dx.doi.org/10.1007/s00531-012-0786-z>.
- Koch, A., 1880. Über das Tertiär in Siebenbürgen. *Neues Jahrbuch für Mineralogie, Geologie und Paläontologie*, I: 283-285.
- Kövecsi, S.A., Silye, L., Less, G., Filipescu, S., 2016. Odd partnership among middle Eocene (Bartonian) *Nummulites*: Examples from the Transylvanian (Romania) and Dorog (Hungary) Basins. *Marine Micropaleontology*, 127: 86-98. <http://dx.doi.org/10.1016/j.marmicro.2016.07.008>.
- Kövecsi, S.A., Zágoršek, K., Filipescu, S., Silye, L., 2018. First report of *Kylonisa triangularis* Keij, 1972 (Bryozoa) from the middle Eocene (Bartonian). *Neues Jahrbuch für Geologie und Paläontologie Abhandlungen*, 289(3): 325-330. <https://doi.org/10.1127/njgpa/2018/0764>.

- Kr zsek, C., Bally, A.W., 2006. The Transylvanian Basin (Romania) and its relation to the Carpathian fold and thrust belt: Insights in gravitational salt tectonics. *Marine and Petroleum*
- Lagaaij, R., Gautier, Y.V., 1965. Bryozoan assemblages from marine sediments of the Rhone delta, France. *Micropaleontology*, 11 (1): 39-58.
- Lamarck, J.B., 1801. *Syst me des animaux sans vert bres, ou tableau g n ral des classes, des ordres et des g bres de ces animaux; Pr sentes leurs caract res essentiels et leur distribution d'apr s la consid ration de leurs rapports naturels et de leur organisation, et suivant l'arrangement  tabli dans les galeries du Mus um d'Histoire Naturelle, parmi leurs d pouilles conserv es; Pr c d  du discours d'ouverture du Cours de Zoologie, donn  dans le Mus um National d'Histoire l'an 8 de la R publique*. Deterville, Paris, 433 pp.
- Lee, J.J., 2006. Algal symbiosis in larger foraminifera. *Symbiosis*, 42(2): 63-75.
- Lee, J.J., Hallock, P., 1987. Algal symbiosis as the driving force in the evolution of larger foraminifera. *Annals of New York Academy of Science*, 503: 330-347. <http://dx.doi.org/10.1111/j.1749-6632.1987.tb40619.x>.
- Lee, J.J., Sang, K., ter Kuile, B., Strauss, E., Lee, P.J., Faber Jr., W.W., 1991. Nutritional and related experiments on laboratory maintenance of three species of symbiont-bearing, large foraminifera. *Marine Biology*, 109: 417-425. <http://dx.doi.org/10.1007/BF01313507>.
- Less, G., Kecskem ti, T., Ozsv rt, P., K zm r, M., B ldi-Beke, M., Koll nyi, K., Fodor, L., Kert sz, B., Varga, I., 2000. Middle-Upper Eocene shallow water benthos in Hungary. *Annali Dell' Universita' Di Ferrara Scienze Terra*, 8: 151-181.
- Leutenegger, S., 1977. Ultrastructure de foraminif res perfor s ainsi que de leurs symbiotes. *Cahiers de Micropal ontologie*, 3:1-52.
- Leutenegger, S., 1984. Symbiosis in benthic foraminifera; specificity and host adaptations. *Journal of Foraminiferal Research*, 14: 16-35. <http://dx.doi.org/10.2113/gsjfr.14.1.16>.
- Levy, A., 1994. Sur un ph nom ne de sp ciation induit par l'environnement chez les Soritidae actuels (Foraminif res). *Oceanological Acta*, 17:33-41.
- Loeblich, A.R., Tappan, H., 1984. Suprageneric classification of the Foraminifera (Protozoa). *Micropaleontology*, 30: 1-70.
- Lowrie, W., Alvarez, W., Napoleone, G., Perch-Nielsen, K., Premoli Silva, I., Toumarkine, M., 1982. Paleogene magnetostratigraphy in Umbrian pelagic carbonate rocks: the Contessa sections, Gubbio. *The Geological Society of America Bulletin*, 93: 414-432.
- Martini, E., 1971. Standard Tertiary and Quaternary calcareous nannoplankton zonation. In: Farinacci, A. (ed.) - *Proceedings 2nd International Conference Planktonic Microfossils Roma*, pp. 739-785.
- McIntyre, A., B , A.W.H., 1967. Modern coccolithophoridae of the Atlantic Ocean – I. *Placoliths and cyrtoliths*. *Deep-Sea Research and Oceanographic*, Abstract 14(5): 561-597.
- Melinte, M.C., 2005. Oligocene palaeoenvironmental changes in the Romanian Carpathians, revealed by calcareous nannoplankton fluctuation. *Annales Societatis Geologicae Poloniae*, 85: 18-28.
- M sz ros N., Moga V., Ianoliu C. 1987. Studying the various groups of fossil organisms of Leghia-Leghia B i. In: Ghergari, L., M sz ros, N., Nicoric, E., Petrescu, I. (eds): - *The Eocene from the Transylvanian Basin Romania*, pp. 143-150.
- M sz ros, N., Moisescu, V., 1991. Bref aper u des unit s lithostratigraphiques du Pal og ne dans le Nord-Ouest de la Transylvanie (r gion de Cluj –Huedin), Roumanie. *Bulletin d'Information des G ologues du Bassin de Paris*, 28(2): 31-39.
- Monechi, S., Buccianti, A., Gardin, S., 2000. Biotic signals from nannoflora across the iridium anomaly in the upper Eocene of the Massignano section: evidence from statistical analysis. *Marine Micropaleontology*, 39: 219-237.
- de Montfort, D., 1808. *Conchyliologie syst matique, et classification m thodique des coquilles*. Tome 1. F. Schoell, Paris, 676 pp. <http://dx.doi.org/10.5962/bhl.title.10571>.
- Murray, J.W., 2006. *Ecology and Applications of Benthic Foraminifera*. Cambridge University Press, pp. 440. <https://doi.org/10.1017/CBO9780511535529>.
- Okada, H., McIntyre, A., 1979. Seasonal distribution of the modern Coccolithophores in the western North Atlantic Ocean. *Marine Biology*, 54(4): 319-328.
- Oszczypko-Clowes, M., 2001. The nannoplankton biostratigraphy of the youngest deposits of the Magura Nappe (east of Skawa River, Polish Flysch Carpathians) and their palaeoenvironmental conditions. *Annales Societatis Geologorum Poloniae*, 71: 139-188.

- Ozdínová, S., Soták, J., 2014. Oligocene–Early Miocene planktonic microbiostratigraphy and paleoenvironments of the South Slovakian Basin (Lučenec Depression). *Geologica Carpathica*, 65: 451-470.
- Papazzoni, C.A., 2008. Preliminary palaeontological observations on some examples of “nummulite banks”: sedimentary or biological origin? *Rendiconti Online Societa Geologica Italiana*, 2: 135–138.
- Papazzoni, C.A., Čosović, V., Briguglio, A., Drobne, K., 2017. Towards a calibrated larger foraminifera biostratigraphic zonation: celebrating 18 years of the application of shallow benthic zones. *Palaios*, 32(1): 1-4. <http://dx.doi.org/10.2110/palo.2016.043>.
- Papazzoni, C.A., Seddighi, M., 2018. What, if anything, is a nummulite bank? *Journal of Foraminifera Research*, 48(4): 276-287. <https://doi.org/10.2113/gsjfr.48.4.276>.
- Papazzoni, C.A., Sirotti, A., 1995. Nummulite biostratigraphy at the Middle-Upper Eocene boundary in the northern Mediterranean area. *Rivista Italiana di Paleontologia e Stratigrafia*, 101(1): 63-80.
- Park, W.C., Schot, E.H., 1968. Stylolites: their nature and origin. *Journal of Sedimentary Petrology*, 38: 175-191. <https://doi.org/10.1306/74D719102B2111D78648000102C1865D>.
- Pecheux, M.J.F., 1995. Ecomorphology of a recent large foraminifer, *Operculina ammonoides*. *Geobios*, 28: 529-566. [http://dx.doi.org/10.1016/S0016-6995\(95\)802096](http://dx.doi.org/10.1016/S0016-6995(95)802096).
- Pleş, G., Kövecsi, S.A., Bindiu-Haitonic, R., Silye, L., 2020. Microfacies analysis and diagenetic features of the Eocene nummulitic accumulations from northwestern Transylvanian Basin (Romania). *Facies*, 66:(3), paper 20. <https://doi.org/10.1007/s10347-020-00604-x>.
- Pop, D., Bedelea, I., 1996. Case histories of some Transylvanian glauconites. *Acta Mineralogica-Petrographica, Szeged*, 37:5-33.
- Popescu, B., 1978. On the lithostratigraphic nomenclature of the NW Transylvania Eocene. *Revue Roumaine de Géologie, Géophysique et Géographie, Géologie*, 22: 99-107.
- Popescu, B., Bombiță, G., Rusu, A., Iva, M., Gheța, N., Olteanu, R., Popescu, D., Tițu, E., 1978. The Eocene of the Cluj - Huedin area. *Dări de Seamă ale Institutului de Geologie și Geofizică*, LXIV(4): 295-357.
- Proust, J.N., Hosu, A., 1996. Sequence stratigraphy and Paleogene tectonic evolution of the Transylvanian Basin (Romania, Eastern Europe). *Sedimentary Geology*, 105: 117-140. [https://doi.org/10.1016/0037-0738\(95\)00144-1](https://doi.org/10.1016/0037-0738(95)00144-1).
- Racey, A., 1995. Lithostratigraphy and larger foraminiferal (nummulitid) biostratigraphy of the tertiary of northern Oman. *Micropaleontology*, 41: 1-123. <http://dx.doi.org/10.2307/1485849>.
- Racey, A., 2001. A review of Eocene nummulite accumulations: structure, formation and reservoir potential. *Journal of Petroleum Geology*, 24: 79-100. <http://dx.doi.org/10.1111/j.1747-5457.2001.tb00662.x>.
- Rahman, A., Roth, P.H., 1990. Late Neogene paleoceanography and paleoclimatology of the Gulf of Aden region based on calcareous nannoplankton. *Paleoceanography*, 5(1): 91-107.
- Răileanu, G., Marinescu, F., Popescu, A., 1968. Harta geologică a Republicii Socialiste România, scara 1:200.000, foaia 27-Târgu Mureș, Comitetul de Stat al Geologiei, Institutul Geologic, Bucharest.
- Răileanu, G., Saulea, E., 1968. Harta geologică a Republicii Socialiste Române, scara 1:200.000, foaia 10-Cluj. Comitetul de Stat al Geologiei, Institutul Geologic, Bucharest.
- Reiss, Z., Hottinger, L., 1984. *The Gulf of Aqaba. Ecological Micropaleontology*. Springer-Verlag, New York, 354 pp. <http://doi.org/10.1007/978-3-642-69787-6>.
- Renema, W., 2005. Depth estimation using diameter-thickness ratios in larger benthic foraminifera. *Lethaia*, 38: 137-141. <http://dx.doi.org/10.1080/00241160510013259>.
- Rozlozsnik, P., 1929. *Studien über Nummulinen*. Geologica Hungarica, Series Paleontologica 2, Institutum Regni Hungariae Geologicum, Budapest, 164 pp.
- Rusu, A., 1987. Ostreina Biohorizons in the Eocene of the North-West Transylvania (Romania). In: Petrescu, I. (ed.) - *The Eocene from the Transylvanian Basin, Romania*. Geological Formations of Transylvania, Romania, 1:175-182.
- Rusu, A., Brotea, D., Melinte, M.C., 2004. Biostratigraphy of the Bartonian deposits from Gilău area (NW Transylvania, Romania). *Acta Palaeontologica Romaniaae*, 4: 441-454.
- Rusu, A., 1995. Eocene formations in the Călata region (NW Transylvania): a critical review. *Romanian Journal of Tectonics and Regional Geology*, 76: 59-72.
- Schaub, H., 1981. *Nummulites et Assilines de la Téthys Paléogène*. Taxinomie, phylogénèse et biostratigraphie. *Schweizerische Paläontologische Abhandlungen*, 104-106: 1-236.

- Schneider, L.J., Bralower, T.J., Kump, L.R., 2011. Response of nannoplankton to early Eocene Ocean deoxygenation. *Palaeogeography, Palaeoclimatology, Palaeoecology*, 310: 152-162.
- Seddighi, M., Briguglio, A., Hohenegger, J., Papazzoni, C.A., 2015. New results on the hydrodynamic behaviour of fossil *Nummulites* tests from two nummulite banks from the Bartonian and Priabonian of northern Italy. *Bollettino della Società Paleontologica Italiana*, 54: 106-116. <http://dx.doi.org/10.4435/BSPI.2015.06>.
- Serra-Kiel J, Reguant S (1984) Paleocological conditions and morphological variations in monospecific banks of *Nummulites*: an example. *Benthos 83, 2nd International Symposium on Benthic Foraminifera* (Pau, 1983), 557-563 pp.
- Serra-Kiel, J., Hottinger, L., Caus, E., Drobne, K., Ferrandez, C., Jauhri, A.K., Less, G. Pavlovec, R., Pignatti, J., Samso, J., M., Schaub, H., Sirel, E., Strougo, A., Tambareau, Y., Tosquella, J., Zakrevskaya, E., 1988. Larger foraminiferal biostratigraphy of the Tethyan Paleocene and Eocene. *Bulletine de la Société Géologique de France*, 2: 281-299.
- Toussaint, R., Aharonov, E., Koehn, D., Gratier, P., Ebner, M., Baud, P., Rolland, A., Renard, F., 2018. Stylolites: A review. *Journal of Structural Geology*, 114: 163-195. <https://doi.org/10.1016/j.jsg.2018.05.003>.
- Tremolada, F., Bralower, T.J., 2004. Nannoplankton assemblage fluctuations during the Paleocene–Eocene thermal Maximum at Sites 213 (Indian Ocean) and 401 (North Atlantic Ocean): palaeoceanographic implications. *Marine Micropaleontology*, 52: 107-116.
- Triantaphyllou, M.V., Dimiza, M.D., Koukousioura, O., Hallock, P., 2012. Observations on the life cycle of the symbiont-bearing foraminifer *Amphistegina lobifera* Larsen, an invasive species in coastal ecosystems of the Aegean Sea (Greece, E. Mediterranean). *Journal of Foraminiferal Research*, 42: 143-150. <http://dx.doi.org/10.2113/gsjfr.42.2.143>.
- Vandeginste, V., John, C.M., 2013. Diagenetic implications of stylolitization in pelagic carbonates, Canterbury Basin, Offshore New Zealand. *Journal of Sedimentary Research*, 83(3): 226-240. <https://doi.org/10.2110/jsr.2013.18>.
- Villa, G., Fioroni, C., Pea, L., Bohaty, S., Persico, D., 2008. Middle Eocene–late Oligocene climate variability: calcareous nannoplankton response at Kerguelen Plateau, Site 748. *Marine Micropaleontology*, 69: 173-192.
- Wanek, F., Mészáros, N., Zotoiu, B. 1987. The Eocene ostracods belonging to the Inferior Marine Series from the North-Western part of the Transylvanian Basin in the light of the Leghia section. In: Ghergari, L., Mészáros, N., Nicoric, E., Petrescu, I. (eds.). *The Eocene from the Transylvanian Basin Romania* pp. 123-126.
- Wei, W., Wise Jr., S.W., 1990. Biogeographic gradients of middle Eocene– Oligocene calcareous nannoplankton in the South Atlantic Ocean. *Palaeogeography, Palaeoclimatology, Palaeoecology*, 79: 29-61.
- Young, J., 1990. Size variation of Neogene Reticulofenestra coccoliths from Indian Ocean DSDP Cores. *Journal of Micropaleontology*, 9(1): 71-86.
- Zachos, J.C., Dickens, G.R., Zeebe, R.E., 2008. An early Cenozoic perspective on greenhouse warming and carbon-cycle dynamics. *Nature*, 451(7176):279-283. <https://doi.org/10.1038/nature06588>.
- Zohary, T., Reiss, Z., Hottinger, L., 1980. Population dynamics of *Amphisorus hemprichii* (foraminifera) in the Gulf of Elat (Aqaba), Red Sea. *Eclogae Geologicae Helvetiae*, 73: 1071-1094. <http://dx.doi.org/10.5169/seals-165002>.